Dorsal root ganglion axon bifurcation tolerates increased cyclic GMP levels: the role of phosphodiesterase 2A and scavenger receptor Npr3

Schmidt, H. and Peters, S. and Frank, K. and Wen, L. and Feil, R. and Rathjen, F.G.

Schmidt, H., Peters, S., Frank, K., Wen, L., Feil, R. and Rathjen, F. G. (2016), Dorsal root ganglion axon bifurcation tolerates increased cyclic GMP levels: the role of phosphodiesterase 2A and scavenger receptor Npr3. Eur J Neurosci, 44: 2991–3000. doi:10.1111/ejn.13434

which has been published in final form in:

European Journal of Neuroscience
2016 DEC; 44(12): 2991-3000
2016 NOV 03 (first published online)
doi: 10.1111/ejn.13434

Publisher: Wiley-Blackwell

Journal section: Developmental Neuroscience

DRG axon bifurcation tolerates increased cGMP levels: the role of phosphodiesterase 2A and scavenger receptor Npr3

Hannes Schmidt [1], Stefanie Peters [2], Katharina Frank [1, 3], Lai Wen [2], Robert Feil [2], and Fritz G. Rathjen [1]

[1] Max-Delbrück-Centrum für Molekulare Medizin in der Helmholtz-Gemeinschaft, 13092 Berlin, Germany
[2] Interfakultäres Institut für Biochemie, University of Tübingen, 72076 Tübingen, Germany
[3] Current address: Institut für Immunologie, BioMedical Center (SFB1054), Ludwig-Maximilians-Universität, 82152 Planegg-Martinsried, Germany

Running title: Role of PDE2A and Npr3 in sensory axon bifurcation

Correspondence: Hannes Schmidt or Fritz G. Rathjen, as above

E-mail: hannes.schmidt@mdc-berlin.de or rathjen@mdc-berlin.de

Total number of words in the whole manuscript: 7642

Total number of words in the abstract: 242

Total number of words in the introduction: 500

Key words: cyclic GMP, CNP, Npr3, Npr2, axon branching, dorsal root ganglion neurons

ABSTRACT

A cGMP signaling pathway, comprising C-type natriuretic peptide (CNP), its guanylate cyclase receptor Npr2, and cGMP-dependent protein kinase I (cGKI), is critical for the bifurcation of dorsal root ganglion (DRG) and cranial sensory ganglion axons when entering the mouse spinal cord and the hindbrain, respectively. However, the identity and functional relevance of phosphodiesterases (PDEs) that degrade cGMP in DRG neurons are not completely understood. Here we asked whether regulation of the intracellular cGMP concentration by PDEs modulates the branching of sensory axons. Real-time imaging of cGMP with a genetically encoded fluorescent cGMP sensor, RT-PCR screens, in situ hybridization, and immunohistology combined with the analysis of mutant mice identified PDE2A as the major enzyme for the degradation of CNP-induced cGMP in embryonic DRG neurons. Tracking of PDE2A-deficient DRG sensory axons in conjunction with cGMP measurements indicated that axon bifurcation tolerates increased cGMP concentrations. Since we found that the natriuretic peptide scavenger receptor Npr3 is expressed by cells associated with dorsal roots but not in DRG neurons itself at early developmental stages, we analyzed axonal branching in the absence of Npr3. In Npr3-deficient mice, the majority of sensory axons showed normal bifurcation, but a small population of axons (13%) was unable to form T-like branches and generated turns in rostral or caudal directions only. Taken together, this study shows that sensory axon bifurcation is insensitive to increases of CNP-induced cGMP levels and Npr3 does not have an important scavenging function in this axonal system.

INTRODUCTION

cGMP is an ubiquitous second messenger involved in a multitude of cellular functions (Kemp-Harper & Feil, 2008). cGMP is synthesized from GTP by heterodimeric NO-sensitive soluble guanylate cyclases or homodimeric transmembrane guanylate cyclases such as Npr2 (Kuhn, 2016). Genetic studies showed that the CNP/Npr2/cGMP pathway regulates endochondral bone growth (Peake *et al.* 2014; Potter 2011b), sensory axon bifurcation (Gibson & Ma 2011; Schmidt & Rathjen 2010), and meiotic prophase arrest during oocyte maturation (Shuhaibar *et al.* 2015; Zhang *et al.* 2010). In humans, biallelic loss-of-function mutations in the Npr2 gene result in acromesomelic dysplasia type Maroteaux (AMDM), a skeletal dysplasia with an extremely short and disproportionate stature (Bartels *et al.* 2004).

Sensory axons from DRGs or cranial ganglia enter the spinal cord or hindbrain, respectively, dorsally and then immediately form a T-like branch. The two stem axons that evolve from the splitting of the growth cone extend over several segments along the lateral margin of the cord or hindbrain. In the absence of the ligand CNP or the receptor Npr2, sensory axons no longer form T-like branches and instead grow only in either rostral or caudal direction (Schmidt *et al.* 2009; Schmidt *et al.* 2007; Ter-Avetisyan *et al.* 2014; Zhao & Ma 2009). Identical branching defects were observed in mutants that lack cGKI indicating that cGKI is the downstream effector of the CNP/Npr2/cGMP pathway (Schmidt *et al.* 2002). Interestingly, studies on human body height regulation indicated that not only complete loss-of-function mutations but also mutations that lead to variations of the CNP level or Npr2 activity can affect skeletal growth (Estrada *et al.* 2009; Olney *et al.* 2012; Potter 2011b). Therefore, it is of interest to clarify whether deregulations of cGMP levels also affect axonal bifurcation within the spinal cord. Branching

errors of even a subpopulation of sensory axons in the spinal cord might affect sensory perception.

cGMP homeostasis is controlled by the rate of its synthesis via guanylate cyclases and degradation via PDEs (Bender & Beavo 2006; Maurice *et al.* 2014; Xu *et al.* 2011). Hydrolysis of cyclic nucleotides by PDEs might prevent the diffusion of cyclic nucleotide signals into neighboring intracellular compartments and, therefore, contribute to the fine-tuning of cGMP signaling.

cGMP signaling is also regulated by the availability of natriuretic peptides in the extracellular milieu, which is dependent on the scavenger receptor Npr3. In chondrocytes, it acts as a clearance receptor by subjecting natriuretic peptides to lysosomal degradation. Deletion of Npr3 in mice results in significant skeletal overgrowth (Matsukawa *et al.* 1999). Therefore, Npr3 might also modulate CNP/Npr2 signaling in DRG neurons.

In the present study, we asked which of the known PDEs hydrolyzes CNP/Npr2-induced cGMP in sensory neurons and whether a deficit of cGMP degradation affects branching of sensory axons. Our studies indicate that PDE2A is important for the hydrolysis of cGMP in embryonic DRGs, that Npr2-mediated axon bifurcation tolerates increased cGMP levels in the absence of PDE2A, and that a subpopulation of sensory axons fails to bifurcate in the absence of the scavenger receptor Npr3.

Materials and methods

FRET-based cGMP imaging in DRG neurons

DRG neurons were isolated from R26-CAG-cGi500(L1) mice that express the cGMP sensor cGi500 globally in all tissues (Thunemann *et al.* 2013b). C57BL/6 female mice were mated with R26-CAG-cGi500 heterozygous male mice. Plug-positive females were separated 0.5 dpc. At day 12.5 dpc pregnant females were euthanized with CO_2 and cGi500 transgenic embryos were used for further preparation. The spinal cord with attached DRGs was dissected from E12.5 embryos and 30-40 DRGs were collected. The DRGs were trypsinized, suspended in DMEM/F12 (Invitrogen) supplemented with 10% horse serum (Life Technologies), 0.3 mg/mL L-glutamine (Life Technologies), 1% penicillin/streptomycin (Invitrogen), 8 mg/mL glucose (Roth), and 100 ng/mL nerve growth factor (Alomone Labs), and plated on poly-D-lysine/laminin-coated coverslips. Cells were grown at 37°C and 6% CO_2 in a humidified incubator.

FRET/cGMP imaging was performed 24 hours after plating using an imaging setup as described previously (Thunemann *et al.* 2013a; Thunemann *et al.* 2013b). Briefly, the imaging setup was based on an inverted Axiovert 200 microscope (Carl Zeiss Microscopy GmbH) equipped with a Plan NeoFluar40×/1.30 oil objective, a light source with excitation filter switching device (Oligochrome, TILL Photonics GmbH), a DualView beam splitter with 516 nm dichroic mirror and emission filters for CFP (480/30 nm) and YFP (535/40 nm) (Photometrics), and a charge-coupled device camera (Retiga 2000R, QImaging). The cells were superfused at room temperature at a flow rate of 1 mL/min with imaging buffer (in mM: NaCl 140, KCl 5, $MgSO_4$ 1.2, $CaCl_2$ 2.5, glucose 5, HEPES 5, pH 7.4) without drugs or with ANP (Tocris), Bay 60-7550

(Santa Cruz), BNP (Phoenix Pharmaceuticals), CNP (Tocris), DEA/NO (Axxora), EHNA (Axxora), IBMX (Sigma Aldrich), milrinone (Santa Cruz), sildenafil (Santa Cruz), vinpocetine (Biomol), or zaprinast (Santa Cruz). For the analysis of FRET data, ImageJ (Schneider *et al.* 2012), Microsoft Excel (Microsoft Corp.), and OriginPro (OriginLab Corp.) software were used. F_{480} and F_{535} traces were background-corrected before calculating the F_{480}/F_{535} ratio R. $\Delta F_{480}/F_{480}$, $\Delta F_{535}/F_{535}$ and $\Delta R/R$ traces were obtained by normalization to the baseline recorded for 2-3 min at the beginning of each experiment (Thunemann *et al.* 2013a). For $\Delta R/R$ peak area calculation, the OriginPro peak area analyzer was used. The peak borders were defined manually.

Statistical analysis

For statistical analysis of PDE inhibitor studies with triple CNP stimulation, a one-way ANOVA was performed for repeated measurements using OriginPro 2015G Software (OriginLab Corporation, Northampton, MA, USA). Results are shown as average of peak area ± SEM. To test for homogeneity of variance the Levene's test was used. Significance testing was carried out using Bonferroni post-hoc test to compare the three individual CNP stimulations. P values <0.05 were considered to be significant. T-test was applied for the pairwise comparison of cGMP concentrations in intact DRGs and for the analysis of axon bifurcation in the absence of PDE2A or Npr3.

cGMP concentrations in intact DRGs

cGMP concentrations in acutely isolated DRGs from wild type or PDE2A-deficient embryos were measured after or without stimulation with 0.5 µM CNP-22 (Calbiochem) by the cGMP Biotrak assay from GE Healthcare as detailed in (Schmidt *et al.* 2009).

Mice

The following mutant mice were used: R26-CAG-cGi500(L1) (Gt(ROSA)26Sor$^{tm1.1(CAG-ECFP/EYFP*)/Feil}$) (Thunemann *et al.* 2013b), Npr2-lacZ (B6.129P2-Npr2$^{tm1.1(nlsLacZ)/Fgr}$ (Ter-Avetisyan *et al.* 2014), PDE2A knockout (B6;129P2-Pde2a$^{tm1Dgen/H}$, obtained from EMMA), Npr3 knockout (B6;129-Npr3$^{tm1Unc/Mmnc}$ obtained from MMRRC) (Matsukawa *et al.* 1999), and Thy1-GFP-M (Tg(Thy1-EGFP)MJrs) (Feng *et al.* 2000). Littermates served as controls. The animal procedures were performed according to the guidelines from directive 2010/63/EU of the European Parliament on the protection of animals used for scientific purposes. All experiments were approved by the local authorities of Berlin (LAGeSo Berlin licence numbers T0313/97 and G0371/13). For FRET-based cGMP imaging studies four C57BL/6 female mice (age 12-24 weeks) were euthanized using CO_2 and for histological studies mice were sacrificed by cervical dislocation and embryos by decapitation. In total, six cGi500 transgenic embryos were used for E12.5 DRG preparation. For the histology in total six adult females and their embryos at E12.5, for binding experiments using AP-CNP-53 two Npr3 heterozygous females and their embryos at E12.5, for cGMP determination eight wild type and three PDE2A heterozygous females with their embryos at E13.5, for bifurcation studies three PDE2A heterozygous females and their embryos at E12.5 and eight Npr3 and three wild type mice and for the RT-PCR studies one female with E12.5 embryos were used.

Immunohistology, expression of a CNP-53 fusion protein, and axon tracing

Paraformaldehyde-fixed cryostat sections (15-µm thick) were stained with the following antibodies: rabbit anti-PDE2A (Santa Cruz, SC-25565, 1:150), rabbit anti-cGKI (Valtcheva *et al.* 2009) (1:1000), chick anti-beta-galactosidase (Abcam, ab9361, 1:5000), rabbit anti-alkaline phosphatase (GenHunter Corp., Q301, 1:2500) or mAb anti-neurofilament (2H3, Developmental Hybridoma Bank, 7.5 µg/ml). Secondary antibodies were applied at the following dilutions: 1:1,000 goat-anti-chick-IgY-Alexa647, 1:1,000 goat-anti-rabbit-Cy3, 1:1,000 goat-anti-rabbit-Alexa647, 1:1,000 goat-anti-mouse-Alexa647 (Dianova).

All microscopic images were obtained at room temperature using either an Axiovert 135 inverted microscope equipped with Neofluar/Acroplan objectives (5x, 10x, or 40x magnification with numerical apertures 0.15, 0.25, or 0.75, respectively), a charge-coupled device camera (Axiocam HRC), and acquisition software (Axiovision 3.1) or by confocal imaging using an Axio Observer.Z1 inverted microscope equipped with ZEN 2011 software and the following lenses: a Plan-Neofluar 10x/0.30 NA objective or a Plan-Achromat 63x/1.40 NA oil objective (all from Carl Zeiss MicroImaging, GmbH). Images were imported into Photoshop CS5 (Adobe) for adjustment of contrast and brightness. Figures were assembled using Illustrator CS5 (Adobe).

As an affinity probe for CNP receptors a chimeric protein termed AP-CNP-53 was produced that consists of the 53 C-terminal amino acid residues of CNP fused at its N-terminus to secreted alkaline phosphatase. The DNA sequence that includes the ORF of CNP was amplified from an E17 whole mouse embryo cDNA library using primers Nppc-Forward and -Reverse (Table S1) and subsequently subcloned into the EcoRV-site of pBluescript II KS (Stratagene). From the resulting plasmid a sequence encoding the 53 C-terminal amino acids of CNP was reamplified

using primers AP-CNP-53 and T3 (Table S1), digested with XhoI, and introduced into the XhoI-site of the pAPtag-5 expression vector (GenHunter Corp.). Expression of AP-CNP-53 in transiently transfected COS7 cells was confirmed by immunoblotting of the supernatant with the following antibodies: rabbit anti-CNP (Peninsula Laboratories Inc., T-4223) and rabbit anti-alkaline phosphatase (GenHunter Corp., Q301). Supernatants were directly applied to paraformaldehyde-fixed spinal cords from E12.5 mouse embryos for 1 hour and binding was visualized by the alkaline phosphatase reaction using the substrates 5-Bromo-4-chloro-3-indolyl phosphate (BCIP) and nitro blue tetrazolium chloride (NBT) (Sigma) according to the protocol by Brennan and Fabes (Brennan & Fabes 2003).

Bifurcation of sensory axons was analyzed by DiI injections or by the reporter mouse Thy-1-GFP-M as detailed elsewhere (Feng *et al.* 2000; Schmidt & Rathjen 2011; Schmidt *et al.* 2007).

RT-PCR and in situ hybridization

RNA from E12.5 mouse DRG was isolated using TRI Reagent (Sigma) according to the manufacturer's instructions. cDNA was synthetized using SuperScript III (Thermo Fisher Scientific). PCR was performed using primers as detailed in table S1 of the supporting information. An E17 whole mouse embryo cDNA library served as a positive control.

For in situ hybridization DNA fragments encoding Pde2A, cGKI and Npr3 were amplified using primers PDE2A-FOR and –REV, Prkg1-FOR and –REV and Npr3-FOR and -REV, respectively, and subcloned into the EcoRV-site of pBluescript II KS (Stratagene) to serve as template for the generation of sense and anti-sense probes. Mouse embryos at E11.5, E12.5 and E13.5 were freshly embedded into OCT compound (Sakura Finetek USA Inc.) and 25 µm transversal sections were processed as previously described (Schmidt *et al.* 2007).

RESULTS

PDE2A degrades cGMP in embryonic DRG neurons

To analyze cGMP levels, real-time imaging experiments were performed by fluorescence resonance energy transfer (FRET) measurements in DRG neurons obtained from transgenic mice that express the genetically encoded FRET-based cGMP sensor, cGi500 (Russwurm *et al.* 2007; Thunemann *et al.* 2013b). DRG neurons from E12.5 embryos were cultivated on laminin1 at low density allowing for the analysis of individual neurons. The cGMP sensor is found to be localized uniformly throughout the neuron including the axon shaft and growth cone (Fig. 1A and C). Since recordings made at the growth cone were less intense the following FRET measurements and quantifications were performed at the cell soma (Fig. 1B and D). Upon application of 100 nM CNP, but not ANP, BNP or the NO donor DEA/NO, the intracellular cGMP level was increased immediately (Fig. 1D), which is in line with our previous studies on intact embryonic DRGs from CNP mutant or wild type mice and which is also in agreement with the pattern of expression of guanylate cyclases in embryonic DRGs (Schmidt *et al.* 2009; Schmidt *et al.* 2007). After removal of CNP, the cGMP level decreased within five minutes to baseline (Fig. 1C and D) suggesting that intracellular cGMP is quickly degraded to GMP by PDEs in DRG neurons. Indeed, the broad-spectrum PDE inhibitor IBMX (100 μM) significantly enhanced CNP-induced cGMP accumulation as compared to CNP alone (Fig. 1E to G).

To analyze the expression of PDEs in embryonic DRG and spinal cord neurons, RT-PCR was performed focusing on known PDEs which specifically hydrolyze cGMP or which are dual

substrate enzymes and degrade both cAMP and cGMP (in total 16 enzymes) (Xu *et al.* 2011). RT-PCR revealed expression of mRNAs of PDE2A, 3A, 3B, 6D, 6G, 9A, 10A, and 11A but not of PDE1A, 1B, 1C, 5A, 6A, 6B, 6C and 6H in embryonic DRGs (Fig. 2). Except for 6A, 6B, 6C and 6H, all tested PDEs were also found in embryonic spinal cord.

Real-time cGMP imaging was used to identify functionally relevant PDEs, which degrade CNP-induced cGMP in DRG neurons. A set of six blockers (Maurice *et al.* 2014) of PDEs, whose mRNAs were detected in DRGs by RT-PCR, was applied before stimulation of DRG neurons with CNP. The PDE blockers alone did not affect the intracellular concentration of cGMP in DRG neurons (see Fig. S1). FRET microscopy showed that CNP-induced cGMP was increased by the PDE2 inhibitors EHNA and Bay 60-7550, while blockers of PDE1 (vinpocetine), PDE3 (milrinone), PDE5 (sildenafil), and PDE5, 6, 9, 10, 11 (zaprinast) did not affect the level of intracellular cGMP (Fig. 3A to F, see also Fig. S1, S2 and table S2).

Next, we measured cGMP levels by an ELISA-based method in DRG extracts prepared from wild type and PDE2A-deficient mice (Fig. 4). In wild type DRGs, we detected with this method a strong cGMP increase upon CNP stimulation when simultaneously the PDE blocker IBMX was applied. In the absence of PDE2A, however, CNP-induced cGMP increases were clearly detectable without blocking PDEs with IBMX. The basal level of cGMP in PDE2A -/- embryonic DRGs is indistinguishable from the wild type situation (Fig. S3). Taken together, our pharmacological and genetic evidence indicated that PDE2A is the major PDE involved in the hydrolysis of CNP-induced cGMP in embryonic DRG neurons and that other PDEs are not able to fully compensate for lacking PDE2A activity.

PDE2A is expressed by embryonic DRG neurons

In situ hybridizations revealed a strong expression of PDE2A mRNA in neurons of DRGs and weak expression in a ventrally localized population of cells in the spinal cord similar to the localization of Npr2 or cGKI mRNA at these stages – two known components implicated in T-branch formation (Fig. 5A and 5E, compare A and E) (Schmidt *et al.* 2007; Schmidt *et al.* 2002). Consistently, immunofluorescence staining of transversal cryostat sections of early embryonic stages, when sensory axons are entering the spinal cord, showed localization of PDE2A in DRG neurons, in the dorsal root and in the dorsal funiculus – a structure which contains DRG axons within the spinal cord – and in a ventrally localized population of the spinal cord (Fig. 5B, compare B and F). Higher magnifications of stained cryostat sections of DRGs showed localization of PDE2A in DRG neurons that also express Npr2 (Fig. 5G) and cGKI (Fig. 5E and F). Within the spinal cord, PDE2A expression was observed in a ventrally localized pool of cells, most likely motoneurons, while other spinal cord cells appeared to be negative for PDE2A (Fig. 5A and B). Overall, this timing and pattern of expression of PDE2A in the somata of DRGs, their axons and spinal cord is very similar to that observed for cGKI and Npr2 at embryonic stages (Schmidt *et al.* 2009; Schmidt *et al.* 2007; Schmidt *et al.* 2002). This localization is also in accordance with hydrolysis of Npr2-generated cGMP by PDE2A.

Three isoforms of PDE2A - PDE2A1, PDE2A2 and PDE2A3 - are encoded by mRNAs with different 5'-regions that result in different amino-terminal regions. Further inclusion of a 62 bp or a 12 bp insert in the 5'- or central region, respectively, results in additional isoforms of PDE2A (see scheme in Fig. 5D). RT-PCR analysis revealed that PDE2A1, PDE2A2 and transcript variant 1 (isoform 6) of PDE2A are expressed in both the embryonic spinal cord and DRGs while PDE2A3 is only faintly expressed in DRGs whereas transcript variant 5 (isoform 5) of PDE2A was undetectable in both tissues (Fig. 5C). PDE2A1 is a soluble form, while PDE2A2 and

PDE2A3 are associated with membranes (Acin-Perez *et al.* 2011; Russwurm *et al.* 2009) suggesting that PDE2A is found in different subcellular compartments of DRG neurons.

Genetic deletion of PDE2A does not affect bifurcation of sensory axons

On the basis of the localization of PDE2A in embryonic DRGs and its involvement in cGMP hydrolysis upon CNP/Npr2 stimulation we investigated branching of sensory axons in the spinal cord in the above mentioned mouse strain deficient for PDE2A. PDE2A-deficient mice do not survive to weaning age for unknown reasons (www.infrafrontier.eu/sites/infrafrontier.eu/files/upload/public/deltagen/DELTAGEN_T1165/). However, the overall structure of the nervous system is not affected by the absence of PDE2A at early developmental stages (see, for example, cross sections of the spinal cord stained by an antibody to neurofilament in Fig. 6A). Analysis of T-branching by DiI tracing at embryonic day 12.5 demonstrated that PDE2A knockout mouse mutants did not reveal branching errors (Fig. 6B). DRG axons showed normal T-like bifurcations and did not form multiple branches in the dorsal root entry zone. Sensory axons extended at lateral regions of the spinal cord as in wild type spinal cords (Fig. 6A) suggesting that the process of bifurcation and extension can tolerate the lack of cGMP degradation by PDE2A.

Role of the scavenger receptor Npr3 in axonal bifurcation

CNP is thought to be cleared from the extracellular space by the scavenger receptor Npr3 (also termed NPR-C), which in turn might affect cGMP levels. Consistently, loss-of-function mutations of Npr3 cause skeletal overgrowth in rodents due to increased levels of CNP in the

extracellular space (Jaubert *et al.* 1999; Matsukawa *et al.* 1999). In situ hybridization revealed expression of Npr3 mRNA in the roof and floor plate of the spinal cord and along the dorsal roots at E12.5 (Fig. 7A), while DRG were negative for Npr3, which is consistent with previously published data (Zhao & Ma 2009). The expression of Npr3 mRNA in the dorsal roots suggests that Schwann cells or their precursors may express Npr3.

Due to a lack of appropriate antibodies that bind to Npr3 in intact tissues a fusion protein, AP-CNP-53 (Fig. 7B), composed of alkaline phosphatase and CNP-53, a proteolytically processed form of CNP, was generated to study the localization of Npr3 protein. This fusion protein binds strongly to Npr3 expressed in heterologous cells whereas binding to Npr2 was below the detection limit in this assay (Fig. S4). In a whole mount preparation of the intact embryonic spinal cord AP-CNP-53 bound to the dorsal roots as well as the roof and floor plate but not to the attached DRGs from wild type mice (Fig. 7C). Only weak or no binding was observed in the dorsal funiculus. The signal was strongly decreased in tissue from Npr3-deficient mice indicating that AP-CNP-53 binding primarily reflected the localization of the Npr3 protein in the dorsal root and roof plate. The lack of binding in the dorsal funiculus of the Npr3 mutant also indicated that this fusion protein binds not or only weakly to Npr2 as also demonstrated for transfected COS7 cells in Fig. S3 of the supporting information. Npr2 is localized in the dorsal funiculus, dorsal root and somata of the DRG neurons (Schmidt *et al.* 2007). Previous studies also indicated high-affinity binding of CNP to Npr3 (Waldman *et al.* 2008). This pattern of expression of Npr3 in the dorsal roots prompted us to trace the branching of sensory axons at the dorsal root entry zone. Despite its strong expression in the dorsal root, the absence of Npr3 did not result in the formation of accessory branches as might be anticipated from its role in the skeletal system where Npr3 acts as scavenger receptor. In contrast, analysis of axonal branching using the reporter mouse Thy1-GFP-M indicated that the majority of axons bifurcate normally in Npr3

knockout mice. Furthermore, no ectopic T-branching was observed in the dorsal roots (Fig. 7D) which might have been assumed in the absence of CNP clearance by the lacking Npr3 in the dorsal roots. Interestingly, a small percentage of axons (13%) was found at all trunk levels not to branch and to turn only in rostral or caudal direction in the absence of Npr3 (Fig. 7D and E).

DISCUSSION

Our cGMP imaging experiments in individual live cells showed that cGMP generation in embryonic DRG neurons is stimulated by CNP but not by ANP, BNP or NO which is consistent with our previously published data on the pattern of expression of guanylate cyclases in embryonic DRGs. These findings complement our previous investigations on the CNP/Npr2 signaling system, which showed an essential role of cGMP signaling for the bifurcation of sensory axons. In the absence of CNP, Npr2 or cGKI, sensory axons are unable to form T-like branches when entering the spinal cord or hindbrain (Schmidt & Rathjen 2010; Schmidt *et al.* 2009; Schmidt *et al.* 2007; Ter-Avetisyan *et al.* 2014; Zhao & Ma 2009). Most likely, T-branching is required for a refined and precise representation of the body within the central nervous system. Our real-time imaging experiments also demonstrated that CNP-induced cGMP is hydrolyzed within minutes in embryonic DRG neurons. Although several PDEs are detected at the level of mRNAs in embryonic DRGs, our pharmacological and genetic analyses indicated that PDE2A is the most relevant enzyme to degrade CNP-induced cGMP in DRG neurons. Accordingly, after application of CNP cGMP levels increased in intact PDE2A-deficient DRGs in the absence of PDE blockers. However, compensatory mechanisms, e.g. upregulation of other PDEs in sensory neurons, cannot be fully excluded to prevent more drastic increases of cGMP levels in the absence of PDE2A. The normal function of cGMP-specific PDEs is to keep cGMP levels in a narrow range of concentrations, which might be essential for restricted activation of cGMP-dependent effector proteins. To our surprise, impaired degradation of cGMP and, hence, increased CNP-induced cGMP concentrations in the absence of PDE2A did not disturb T-branching of sensory axons, for example, by repeated T-like branching at the dorsal root entry

zone or by affecting overall pathfinding of the growth cone. It appears that sensory axon bifurcation and extension tolerates an increased intracellular cGMP level upon CNP stimulation. Up to now, only loss-of-function mutations of cGMP pathway components in DRG neurons have been shown to cause defects in sensory axon bifurcation. This is remarkable since increasing levels of CNP or Npr2 activity have been reported to affect human body height. For example, heterozygous gain-of-function mutations of Npr2 (Hannema *et al.* 2013; Miura *et al.* 2012; Robinson *et al.* 2013) or balanced translocations in chromosome 2 near the locus of the *Nppc* gene, resulting in overproduction of CNP, cause a tall stature in humans (Bocciardi *et al.* 2007; Moncla *et al.* 2007).

Overall, it might be speculated that an immediate degradation of cGMP in DRGs by PDE2A in the wild type might be required to prevent a spreading of cGMP generated by Npr2 to other cGMP-dependent signaling systems in other cellular compartments. A fast degradation might be important to maintain compartmentalization of cGMP-dependent signaling events. PDE2A hydrolyzes cGMP and cAMP with approximately equal efficiency allowing a negative crosstalk on intracellular cAMP signaling pathways (Zaccolo & Movsesian 2007). It is generally thought that cGMP and cAMP signaling pathways are connected in a complex network including a precise spatial organization, and cGMP regulates cAMP signaling by activating or inhibiting cAMP-degrading PDEs (Zaccolo & Movsesian 2007). Previous *in vitro* experiments using organotypic slice cultures or growth cone turning assays revealed a link between cAMP and cGMP signaling in growth cone extension and steering (Heine *et al.* 2013; Song *et al.* 1998; Tojima *et al.* 2011). Our results show that PDE2A-mediated cyclic nucleotide crosstalk is not required for sensory axons to branch or to grow correctly into the spinal cord *in vivo*.

At more advanced developmental stages, PDE2A expression has a widespread distribution in the central nervous system including the limbic system, olfactory cortex, amygdala and hippocampus

(Van Staveren *et al.* 2003). Our study does not exclude roles of PDE2 in brain functions such as memory formation, inflammatory pain processing, and synaptic plasticity (Fernandez-Fernandez *et al.* 2015; Hu *et al.* 2012; Kallenborn-Gerhardt *et al.* 2014; Redrobe *et al.* 2014; Zhang *et al.* 2015).

Our studies with Npr3-deficient mice further support the notion that bifurcation of sensory axons at the dorsal root entry zone is not disturbed by elevated cGMP levels. In regard to the skeletal system, absence of the scavenger receptor Npr3 causes skeletal overgrowth by increased endochondral ossification due to a reduced clearance of CNP from the extracellular milieu through Npr3 receptor-mediated internalization (Jaubert *et al.* 1999; Matsukawa *et al.* 1999). Thus, in Npr3-deficient mice one might expect an increase of the extracellular CNP concentration in the dorsal spinal cord or dorsal roots leading to a higher number of T-branches or ectopic branching already in the dorsal root before axons are entering the spinal cord. However, contrary to our expectations, genetic deletion of Npr3 led to an impairment of T-branching in only a small fraction of 13% of sensory axons. Apparently, the potential scavenger function of Npr3 for CNP is not functionally relevant for the majority of sensory axons in dorsal roots. Specifically, absence of Npr3 does not impair CNP/Npr2 signaling in these axons when forming T-branches at the dorsal root entry zone. As discussed by others (Potter *et al.* 2006), Npr3, which lacks an intracellular guanylate cyclase domain, might also have a signaling function that is currently unknown for dorsal root cells. The absence of Npr3 expression in DRG axons and its expression only in cells of the dorsal root at early developmental stages suggests that, in contrast to chondrocytes, Npr3 is not directly linked to the CNP/Npr2 signaling system in the DRG neurons. The reasons for the deficits in axon branching in 13% of the sensory neurons in Npr3-deficient mice are currently unknown but might have a secondary origin associated with the overall overgrowth defects of this mutant (Matsukawa *et al.* 1999).

In summary our investigations on the system of axonal T-branching indicate that PDE2A is essential for efficient hydrolysis of cGMP in embryonic DRG neurons, that variations in cGMP levels caused by the absence of PDE2A do not interfere with proper axon bifurcation, and that the influence of the scavenger receptor Npr3 on sensory axon bifurcation is limited to a minor degree. Since bifurcation apparently tolerates high cGMP concentrations, it is unlikely that human patients with variations of PDE2A activity show bifurcation errors of sensory axons.

Acknowledgements

The technical help of Madlen Driesner, Karola Bach, and Barbara Birk is greatly acknowledged. We thank Moritz Lehners, Shen Lu, and Achim Schmidtko for their contributions to the cGMP imaging studies. The generation of the PDE2A mouse line was supported by the Wellcome Trust. We thank Drs Lincoln R. Potter (University of Minnesota) and Erick Miranda from the lab of Michaela Kuhn (University of Würzburg) for providing the Npr3 expression plasmid. This work was supported by DFG grants SFB 665 and FOR 2060 (FE 438/5-1, FE 438/6-1, and SCHM 2371/1).

Conflict of interest

The authors have no conflicts of interest to disclose.

Abbreviations

cGKI, cGMP-dependent kinase I; CNP, C-type natriuretic peptide; DRG, dorsal root ganglion; Npr2, natriuretic peptide receptor 2; Npr3, natriuretic peptide receptor 3; ORF, open reading frame; PDE, phosphodiesterase

References

Acin-Perez,R., Russwurm,M., Gunnewig,K., Gertz,M., Zoidl,G., Ramos,L., Buck,J., Levin,L.R., Rassow,J., Manfredi,G. & Steegborn,C. (2011) A phosphodiesterase 2A isoform localized to mitochondria regulates respiration. *J.Biol.Chem.*, **286**, 30423-30432.

Bartels,C.F., Bukulmez,H., Padayatti,P., Rhee,D.K., Ravenswaaij-Arts,C., Pauli,R.M., Mundlos,S., Chitayat,D., Shih,L.Y., Al Gazali,L.I., Kant,S., Cole,T., Morton,J., Cormier-Daire,V., Faivre,L., Lees,M., Kirk,J., Mortier,G.R., Leroy,J., Zabel,B., Kim,C.A., Crow,Y., Braverman,N.E., van den,A.F. & Warman,M.L. (2004) Mutations in the transmembrane natriuretic peptide receptor NPR-B impair skeletal growth and cause acromesomelic dysplasia, type Maroteaux. *Am.J.Hum.Genet.*, **75**, 27-34.

Bender,A.T. & Beavo,J.A. (2006) Cyclic nucleotide phosphodiesterases: molecular regulation to clinical use. *Pharmacol.Rev.*, **58**, 488-520.

Bocciardi,R., Giorda,R., Buttgereit,J., Gimelli,S., Divizia,M.T., Beri,S., Garofalo,S., Tavella,S., Lerone,M., Zuffardi,O., Bader,M., Ravazzolo,R. & Gimelli,G. (2007) Overexpression of the C-type natriuretic peptide (CNP) is associated with overgrowth and bone anomalies in an individual with balanced t(2;7) translocation. *Hum.Mutat.*, **28**, 724-731.

Brennan,C. & Fabes,J. (2003) Alkaline phosphatase fusion proteins as affinity probes for protein localization studies. *Sci.STKE.*, **2003**, L2.

Estrada,K., Krawczak,M., Schreiber,S., van,D.K., Stolk,L., van Meurs,J.B., Liu,F., Penninx,B.W., Smit,J.H., Vogelzangs,N., Hottenga,J.J., Willemsen,G., de Geus,E.J., Lorentzon,M., von Eller-Eberstein,H., Lips,P., Schoor,N., Pop,V., de,K.J., Hofman,A., Aulchenko,Y.S., Oostra,B.A., Ohlsson,C., Boomsma,D.I., Uitterlinden,A.G., van Duijn,C.M., Rivadeneira,F. & Kayser,M. (2009) A genome-wide association study of northwestern Europeans involves the C-type natriuretic peptide signaling pathway in the etiology of human height variation. *Hum.Mol.Genet.*, **18**, 3516-3524.

Feng,G., Mellor,R.H., Bernstein,M., Keller-Peck,C., Nguyen,Q.T., Wallace,M., Nerbonne,J.M., Lichtman,J.W. & Sanes,J.R. (2000) Imaging neuronal subsets in transgenic mice expressing multiple spectral variants of GFP. *Neuron*, **28**, 41-51.

Fernandez-Fernandez,D., Rosenbrock,H. & Kroker,K.S. (2015) Inhibition of PDE2A, but not PDE9A, modulates presynaptic short-term plasticity measured by paired-pulse facilitation in the CA1 region of the hippocampus. *Synapse*, **69**, 484-496.

Gibson,D.A. & Ma,L. (2011) Developmental regulation of axon branching in the vertebrate nervous system. *Development*, **138**, 183-195.

Hannema,S.E., van Duyvenvoorde,H.A., Premsler,T., Yang,R.B., Mueller,T.D., Gassner,B., Oberwinkler,H., Roelfsema,F., Santen,G.W., Prickett,T., Kant,S.G., Verkerk,A.J., Uitterlinden,A.G., Espiner,E., Ruivenkamp,C.A., Oostdijk,W., Pereira,A.M., Losekoot,M., Kuhn,M. & Wit,J.M. (2013) An activating mutation in the kinase homology domain of the natriuretic peptide receptor-2 causes extremely tall stature without skeletal deformities. *J Clin.Endocrinol.Metab*, **98**, E1988-E1998.

Heine,C., Sygnecka,K., Scherf,N., Berndt,A., Egerland,U., Hage,T. & Franke,H. (2013) Phosphodiesterase 2 inhibitors promote axonal outgrowth in organotypic slice co-cultures. *Neurosignals.*, **21**, 197-212.

Hu,F., Ren,J., Zhang,J.E., Zhong,W. & Luo,M. (2012) Natriuretic peptides block synaptic transmission by activating phosphodiesterase 2A and reducing presynaptic PKA activity. *Proc.Natl.Acad.Sci.U.S.A*, **109**, 17681-17686.

Jaubert,J., Jaubert,F., Martin,N., Washburn,L.L., Lee,B.K., Eicher,E.M. & Guenet,J.L. (1999) Three new allelic mouse mutations that cause skeletal overgrowth involve the natriuretic peptide receptor C gene (Npr3). *Proc.Natl.Acad.Sci.U.S A*, **96**, 10278-10283.

Kallenborn-Gerhardt,W., Lu,R., Bothe,A., Thomas,D., Schlaudraff,J., Lorenz,J.E., Lippold,N., Real,C.I., Ferreiros,N., Geisslinger,G., Del,T.D. & Schmidtko,A. (2014) Phosphodiesterase 2A localized in the spinal cord contributes to inflammatory pain processing. *Anesthesiology*, **121**, 372-382.

Kemp-Harper,B. & Feil,R. (2008) Meeting report: cGMP matters. *Sci.Signal.*, **1**, e12.

Kuhn,M. (2016) Molecular Physiology of Membrane Guanylyl Cyclase Receptors. *Physiol Rev.*, **96**, 751-804.

Matsukawa,N., Grzesik,W.J., Takahashi,N., Pandey,K.N., Pang,S., Yamauchi,M. & Smithies,O. (1999) The natriuretic peptide clearance receptor locally modulates the physiological effects of the natriuretic peptide system. *Proc.Natl.Acad.Sci.U.S A*, **96**, 7403-7408.

Maurice,D.H., Ke,H., Ahmad,F., Wang,Y., Chung,J. & Manganiello,V.C. (2014) Advances in targeting cyclic nucleotide phosphodiesterases. *Nat.Rev.Drug Discov.*, **13**, 290-314.

Miura,K., Namba,N., Fujiwara,M., Ohata,Y., Ishida,H., Kitaoka,T., Kubota,T., Hirai,H., Higuchi,C., Tsumaki,N., Yoshikawa,H., Sakai,N., Michigami,T. & Ozono,K. (2012) An overgrowth disorder associated with excessive production of cGMP due to a gain-of-function mutation of the natriuretic peptide receptor 2 gene. *PLoS.One.*, **7**, e42180.

Moncla,A., Missirian,C., Cacciagli,P., Balzamo,E., Legeai-Mallet,L., Jouve,J.L., Chabrol,B., Le,M.M., Plessis,G., Villard,L. & Philip,N. (2007) A cluster of translocation breakpoints in 2q37 is associated with overexpression of NPPC in patients with a similar overgrowth phenotype. *Hum.Mutat.*, **28**, 1183-1188.

Olney,R.C., Permuy,J.W., Prickett,T.C., Han,J.C. & Espiner,E.A. (2012) Amino-terminal propeptide of C-type natriuretic peptide (NTproCNP) predicts height velocity in healthy children. *Clin.Endocrinol.(Oxf)*, **77**, 416-422.

Peake,N.J., Hobbs,A.J., Pingguan-Murphy,B., Salter,D.M., Berenbaum,F. & Chowdhury,T.T. (2014) Role of C-type natriuretic peptide signalling in maintaining cartilage and bone function. *Osteoarthritis.Cartilage.*, **22**, 1800-1807.

Potter,L.R. (2011a) Guanylyl cyclase structure, function and regulation. *Cell Signal.*, **23**, 1921-1926.

Potter,L.R. (2011b) Regulation and therapeutic targeting of peptide-activated receptor guanylyl cyclases. *Pharmacol.Ther.*, **130**, 71-82.

Potter,L.R., Abbey-Hosch,S. & Dickey,D.M. (2006) Natriuretic peptides, their receptors, and cyclic guanosine monophosphate-dependent signaling functions. *Endocr.Rev.*, **27**, 47-72.

Redrobe,J.P., Jorgensen,M., Christoffersen,C.T., Montezinho,L.P., Bastlund,J.F., Carnerup,M., Bundgaard,C., Lerdrup,L. & Plath,N. (2014) In vitro and in vivo characterisation of Lu AF64280, a novel, brain penetrant phosphodiesterase (PDE) 2A inhibitor: potential relevance to cognitive deficits in schizophrenia. *Psychopharmacology (Berl)*, **231**, 3151-3167.

Robinson,J.W., Dickey,D.M., Miura,K., Michigami,T., Ozono,K. & Potter,L.R. (2013) A human skeletal overgrowth mutation increases maximal velocity and blocks desensitization of guanylyl cyclase-B. *Bone*, **56**, 375-382.

Russwurm,C., Zoidl,G., Koesling,D. & Russwurm,M. (2009) Dual acylation of PDE2A splice variant 3: targeting to synaptic membranes. *J.Biol.Chem.*, **284**, 25782-25790.

Russwurm,M., Mullershausen,F., Friebe,A., Jager,R., Russwurm,C. & Koesling,D. (2007) Design of fluorescence resonance energy transfer (FRET)-based cGMP indicators: a systematic approach. *Biochem.J*, **407**, 69-77.

Schmidt,H. & Rathjen,F.G. (2010) Signalling mechanisms regulating axonal branching in vivo. *Bioessays*, **32**, 977-985.

Schmidt,H. & Rathjen,F.G. (2011) DiI-labeling of DRG neurons to study axonal branching in a whole mount preparation of mouse embryonic spinal cord. *J.Vis.Exp.*, e3667 , DOI: 10.3791/3667.

Schmidt,H., Stonkute,A., Juttner,R., Koesling,D., Friebe,A. & Rathjen,F.G. (2009) C-type natriuretic peptide (CNP) is a bifurcation factor for sensory neurons. *Proc.Natl.Acad.Sci.U.S.A*, **106**, 16847-16852.

Schmidt,H., Stonkute,A., Juttner,R., Schaffer,S., Buttgereit,J., Feil,R., Hofmann,F. & Rathjen,F.G. (2007) The receptor guanylyl cyclase Npr2 is essential for sensory axon bifurcation within the spinal cord. *J.Cell Biol.*, **179**, 331-340.

Schmidt,H., Werner,M., Heppenstall,P.A., Henning,M., More,M.I., Kuhbandner,S., Lewin,G.R., Hofmann,F., Feil,R. & Rathjen,F.G. (2002) cGMP-mediated signaling via cGKIalpha is required for the guidance and connectivity of sensory axons. *J Cell Biol.*, **159**, 489-498.

Schneider,C.A., Rasband,W.S. & Eliceiri,K.W. (2012) NIH Image to ImageJ: 25 years of image analysis. *Nat.Methods*, **9**, 671-675.

Shuhaibar,L.C., Egbert,J.R., Norris,R.P., Lampe,P.D., Nikolaev,V.O., Thunemann,M., Wen,L., Feil,R. & Jaffe,L.A. (2015) Intercellular signaling via cyclic GMP diffusion through gap junctions restarts meiosis in mouse ovarian follicles. *Proc.Natl.Acad.Sci.U.S.A*, **112**, 5527-5532.

Song,H., Ming,G., He,Z., Lehmann,M., McKerracher,L., Tessier-Lavigne,M. & Poo,M. (1998) Conversion of neuronal growth cone responses from repulsion to attraction by cyclic nucleotides. *Science*, **281**, 1515-1518.

Ter-Avetisyan,G., Rathjen,F.G. & Schmidt,H. (2014) Bifurcation of axons from cranial sensory neurons is disabled in the absence of Npr2-induced cGMP signaling. *J Neurosci.*, **34**, 737-747.

Thunemann,M., Fomin,N., Krawutschke,C., Russwurm,M. & Feil,R. (2013a) Visualization of cGMP with cGi biosensors. *Methods Mol.Biol.*, **1020**, 89-120.

Thunemann,M., Wen,L., Hillenbrand,M., Vachaviolos,A., Feil,S., Ott,T., Han,X., Fukumura,D., Jain,R.K., Russwurm,M., de,W.C. & Feil,R. (2013b) Transgenic mice for cGMP imaging. *Circ.Res.*, **113**, 365-371.

Tojima,T., Hines,J.H., Henley,J.R. & Kamiguchi,H. (2011) Second messengers and membrane trafficking direct and organize growth cone steering. *Nat.Rev.Neurosci.*, **12**, 191-203.

Valtcheva,N., Nestorov,P., Beck,A., Russwurm,M., Hillenbrand,M., Weinmeister,P. & Feil,R. (2009) The commonly used cGMP-dependent protein kinase type I (cGKI) inhibitor Rp-8-Br-PET-cGMPS can activate cGKI in vitro and in intact cells. *J.Biol.Chem.*, **284**, 556-562.

Van Staveren,W.C., Steinbusch,H.W., Markerink-Van,I.M., Repaske,D.R., Goy,M.F., Kotera,J., Omori,K., Beavo,J.A. & De,V.J. (2003) mRNA expression patterns of the cGMP-hydrolyzing phosphodiesterases types 2, 5, and 9 during development of the rat brain. *J.Comp Neurol.*, **467**, 566-580.

Waldman,S.D., Usmani,Y., Tse,M.Y. & Pang,S.C. (2008) Differential effects of natriuretic peptide stimulation on tissue-engineered cartilage. *Tissue Eng Part A*, **14**, 441-448.

Xu,Y., Zhang,H.T. & O'Donnell,J.M. (2011) Phosphodiesterases in the central nervous system: implications in mood and cognitive disorders. *Handb.Exp.Pharmacol.*, 447-485.

Zaccolo,M. & Movsesian,M.A. (2007) cAMP and cGMP signaling cross-talk: role of phosphodiesterases and implications for cardiac pathophysiology. *Circ.Res.*, **100**, 1569-1578.

Zhang,C., Yu,Y., Ruan,L., Wang,C., Pan,J., Klabnik,J., Lueptow,L., Zhang,H.T., O'Donnell,J.M. & Xu,Y. (2015) The roles of phosphodiesterase 2 in the central nervous and peripheral systems. *Curr.Pharm.Des*, **21**, 274-290.

Zhang,M., Su,Y.Q., Sugiura,K., Xia,G. & Eppig,J.J. (2010) Granulosa cell ligand NPPC and its receptor NPR2 maintain meiotic arrest in mouse oocytes. *Science*, **330**, 366-369.

Zhao,Z. & Ma,L. (2009) Regulation of axonal development by natriuretic peptide hormones. *Proc.Natl.Acad.Sci.U.S.A*, **106**, 18016-18021.

Figure Legends

Figure 1

FRET-based cGMP imaging in individual DRG neurons from R26-CAG-cGi500 (L1) mice.

(A) Representative image of an E12.5 DRG growth cone expressing the cGMP sensor cGi500 (shown in green). A DRG explant culture was prepared to test the CNP stimulus on DRG growth cones. DRGs from R26-CAG-cGi500(L1) were isolated (see materials and methods), cut in half and transferred to the culture dish. Scale bar 10 µm. (B) Measurements were started 24 h after plating. FRET-based cGMP imaging was performed with perfusion of 100 nM CNP (black horizontal bar). Signals were recorded from the growth cone. Traces indicate CFP emission (F480), YFP emission (F535), and the CFP/YFP emission ratio (R=F480/F535). Emission intensities and ratios were normalized to averaged baseline signals and are given as ΔF/F and ΔR/R, respectively. (C) Expression of the cGi500 biosensor in a DRG neuron cultivated in a monolayer from E12.5 embryos 24 hours after plating. Scale bar, 20 µm. (D) FRET-based cGMP imaging was performed with perfusion of drugs (horizontal bars) in the following order: 100 nM DEA/NO, 100 nM ANP, 100 nM BNP, and 100 nM CNP. Signals were recorded from the soma. Traces indicate CFP emission (F480), YFP emission (F535), and the CFP/YFP emission ratio (R=F480/F535). Emission intensities and ratios were normalized to averaged baseline signals and are given as ΔF/F and ΔR/R, respectively. Note that changes of ΔR/R indicate changes of the intracellular cGMP concentration. Based on in-cell calibration of cGi500 in permeabilized vascular smooth muscle cells (Thunemann *et al.* 2013a), the peak of the CNP-induced cGMP transient in

E12.5 DRG neurons corresponds to ~0.5 µM cGMP. Representative results from ≥ 3 experiments with independent cell cultures are shown.

(E-G) The broad-spectrum PDE inhibitor IBMX potentiates the CNP-induced cGMP signal in DRG neurons. (E and F) FRET-based cGMP imaging was performed in cells that were superfused three times with 100 nM CNP (black horizontal bars in panel F), with the second CNP application in presence of 100 µM IBMX (red horizontal bar in panel F). Signals were recorded from the soma. Changes of ΔR/R reflect changes of the intracellular cGMP concentration. The signals at time points t_0-t_3 indicated in panel F correspond to the pictures shown in panel E. (F) Compared to baseline (t_0), stimulation with 100 nM CNP (t_1) leads to an elevation of the CFP/YFP emission ratio (R=F480/F535) that correlates with the intracellular cGMP concentration. After preincubation with IBMX, CNP stimulation (t2) results in ~2.5 times higher peak cGMP concentrations as compared to CNP alone. After washout of IBMX, the third CNP application (t_3) leads to an increase of the cGMP concentration that is comparable to the first stimulation. Scale bar, 20 µm. (G) Summary of CNP-induced cGMP signals before, during and after incubation with IBMX. Peak areas were taken as a measure of the cGMP response and normalized to the first peak of the experiment. Data are mean±SEM (n = 6 cells); ***p<0.001.

Figure 2

Several PDEs are expressed in embryonic DRGs and spinal cord.

(A and B) RT-PCR screen of cGMP-specific and dual substrate-specific PDEs expressed in E12.5 DRGs or spinal cord (SC). For comparison amplification products of Npr2 and cGKIα are shown in A). The sizes of the PCR amplification products are given in parenthesis. – no template in the reaction mixture, + amplification from an embryonic mouse cDNA library.

Figure 3

Pharmacological profiling of PDE activities in DRG neurons.

FRET-based cGMP imaging was used to determine the effects of various PDE inhibitors on CNP-induced cGMP signals as described in the legend to Figure 1. Cells were stimulated three times with 100 nM CNP. The second CNP stimulation was done after preincubation of the cells for 5 min with (A) 5μM vinpocetine (Vin), (B) 10 nM Bay 60-7550 (Bay), (C) 10 μM EHNA, 10 μM milrinone (Mil), (E) 20 μM sildenafil (Sil), or (F) 20 μM zaprinast (Zap). The specificity of each PDE inhibitor is indicated above each diagram. Signals were recorded from the soma. Peak areas were taken as a measure of the cGMP response and normalized to the first peak of each experiment. Data are mean±SEM (n cells in the experiment as indicated in the respective panel at the right); ***$p<0.001$; *$p<0.05$.

Figure 4

PDE2A degrades CNP-induced cGMP.

Intact DRGs from wild type, PDE2A heterozygote or homozygous knockout mice were incubated with or without CNP-22 (0.5 μM) for 15 minutes at 37^{o}C in the presence or absence of IBMX (1 mM). The cGMP concentration in DRG extracts was determined by an ELISA-based method as described in (Schmidt *et al.* 2009). Values are mean±SEM; numbers above columns indicate numbers of independent DRG preparations; t-tests were performed to compare the mean difference of two groups;*** $p<0.001$, n.s., non-significant.

Figure 5

Analysis of PDE2A expression in embryonic DRGs and spinal cords.

A) In situ hybridization of transverse sections of the spinal cord and DRGs with a PDE2A sense (S) or antisense (AS) probe reveals expression of PDE2A in DRGs and a ventrally localized pool of cells of the spinal cord. Scale bar, 200 µm. B) Immunostaining of transverse sections of the spinal cord and DRGs showing expression of PDE2A protein in DRGs, dorsal funiculus and a ventrally localized group of cells of the spinal cord. Scale bar, 200 µm. C) RT-PCR detection of PDE2A isoforms expressed in embryonic DRGs and spinal cord (SC). – no template in the reaction mixture, + amplification from an embryonic mouse cDNA library. TV, transcript variant; IF, isoform. D) Scheme of the different isoforms of PDE2A. E and F) for comparison, ISH of cGKI anti-sense probe and immunostaining of cGKI is shown. Scale bar, 200 µm. Broken lines in E) indicate the margin of the spinal cord and the DRG. G) Higher magnification of sections from an *Npr2*$^{LacZ/+}$ reporter mouse indicates expression of PDE2A in Npr2-positive DRG neurons with nuclear labelling by an antibody to β-galactosidase. Scale bar, 10 µm.

Figure 6

Analysis of sensory axon bifurcation in PDE2A mutant mice by DiI tracing.

A) Transversal sections of embryonic spinal cord stained with antibodies to neurofilament (NF-M) indicate that the overall structure of PDE2A-deficient spinal cord is indistinguishable from wild type spinal cord. Scale bar, 100 µm. B) DiI tracing shows that bifurcation of sensory axons is not impaired in the absence of PDE2A. 402 and 317 DRG axons were

counted for wild type and for PDE2A -/-, respectively. In the right panel several PDE2A-deficient bifurcating sensory axons were labeled by DiI that are located behind the front axon. T-test indicates that the percentage of bifurcating axons in the wild type and PDE2A -/- are indistinguishable (wild type n = 3, PDE2A -/- n = 3, p = 0.123). Scale bar, 25 μm. C) Scheme of T-branching of sensory axons in the spinal cord. Sensory axons enter the spinal cord at the so-called dorsal root entry zone, bifurcate (indicated by an A) and extend at the lateral margin of the spinal cord over several segments. At more advanced stages, these stem axons form collaterals (indicated by a B) that grow to dorsal or ventral target regions of the cord where terminal branching occurs (indicated by a C).

Figure 7

Localization of Npr3 in the spinal cord and analysis of its role in axon bifurcation.

A) In situ hybridization using antisense (AS) and sense (S) probes to monitor Npr3 expression in transversal sections of the spinal cord reveal localization of Npr3 mRNA in the floor plate (FP), roof plate (RP) and dorsal root (DR) but not in DRGs itself. Broken lines indicate the margin of the spinal cord and the DRG. B) Expression of alkaline phosphatase (AP) or a fusion protein composed of CNP-53 and alkaline phosphatase (AP-CNP-53) in transiently tranfected COS7 cells followed by Western blotting of the resultant conditioned media using antibodies to the alkaline phosphatase (upper panel, Rb-a-AP) or to CNP (lower panel, Rb-a-CNP). The left and right lanes show expression of the alkaline phosphatase or of the fusion protein, respectively. Molecular mass standards are indicated at the right of the panels.

C) Detection CNP receptors in a whole-mount preparation of embryonic spinal cord using a fusion protein of CNP-53 and alkaline phosphatase (AP-CNP-53). Dorsal views demonstrate binding in dorsal roots (DR) and the roof plate (RP) of wild type embryos (upper panel), but not or only very weakly in the corresponding structures of Npr3-deficient embryos (lower panel). No staining was observed in controls with alkaline phosphatase alone (not shown). (D and E) Analysis of axon bifurcation in Npr3 knockouts crossed to the reporter mouse Thy-1-GFP-M. Spinal cords with attached DRGs were prepared at postnatal day 30 (P30). No ectopic bifurcation outside the DREZ were detected in the absence of Npr3. Arrows indicate bifurcations, arrow heads show turns in rostral or caudal directions and demonstrate the absence of bifurcations. In total 754 and 982 DRG axons were counted for wild type and Npr3-/- mutants, respectively. T-test indicates that wild type and Npr3 -/- are significantly distinct from each other (wild type $n = 3$, Npr3 -/- $n = 8$, $p<0.001$).

Figure 1

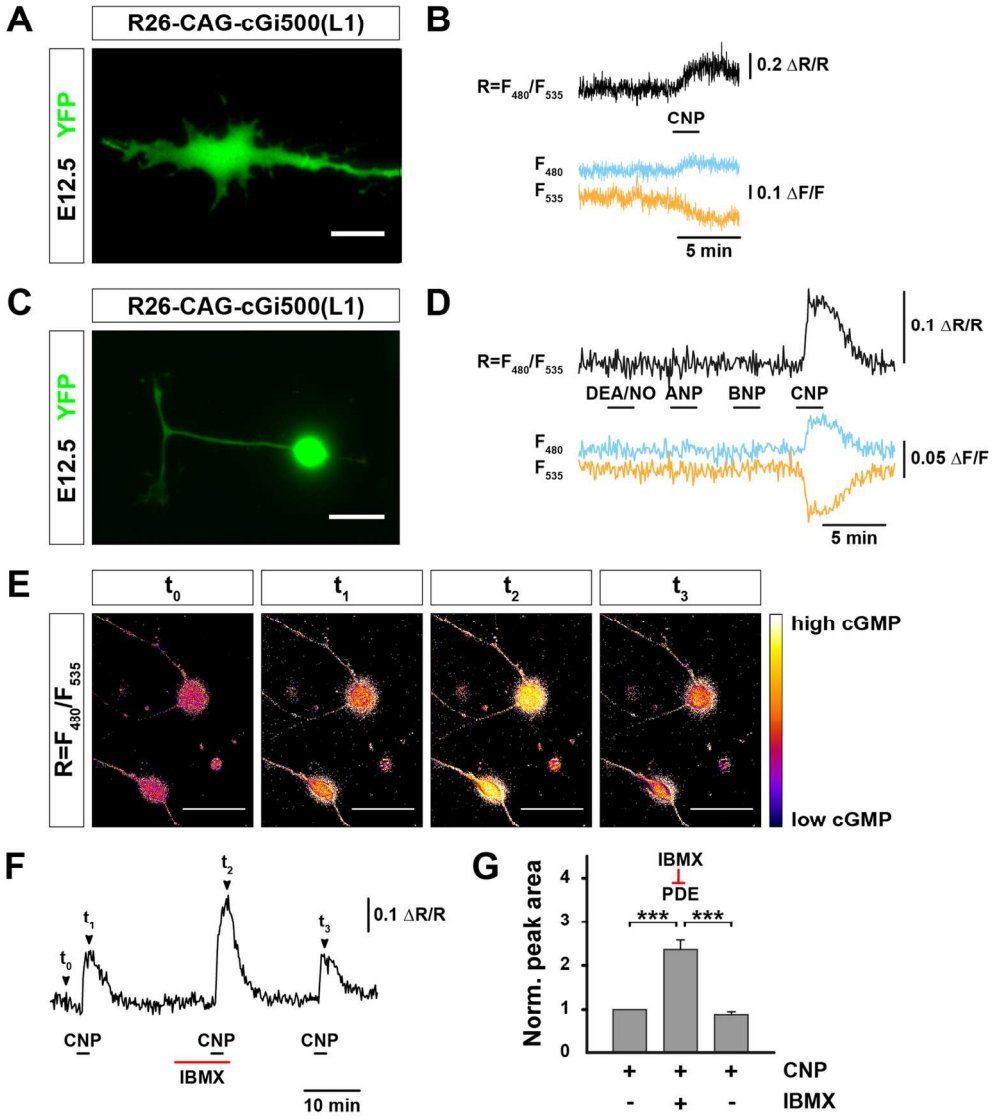

Fig. 1:

FRET-based cGMP imaging in individual DRG neurons from R26-CAG-cGi500 (L1) mice.

(A) Representative image of an E12.5 DRG growth cone expressing the cGMP sensor cGi500 (shown in green). A DRG explant culture was prepared to test the CNP stimulus on DRG growth cones. DRGs from R26-CAG-cGi500(L1) were isolated (see materials and methods), cut in half and transferred to the culture dish. Scale bar 10 µm. (B) Measurements were started 24 h after plating. FRET-based cGMP imaging was performed with perfusion of 100 nM CNP (black horizontal bar). Signals were recorded from the growth cone. Traces indicate CFP emission (F480), YFP emission (F535), and the CFP/YFP emission ratio (R=F480/F535). Emission intensities and ratios were normalized to averaged baseline signals and are given as ΔF/F and ΔR/R, respectively. (C) Expression of the cGi500 biosensor in a DRG neuron cultivated in a monolayer from E12.5 embryos 24 hours after plating. Scale bar, 20 µm. (D) FRET-based cGMP imaging

was performed with perfusion of drugs (horizontal bars) in the following order: 100 nM DEA/NO, 100 nM ANP, 100 nM BNP, and 100 nM CNP. Signals were recorded from the soma. Traces indicate CFP emission (F480), YFP emission (F535), and the CFP/YFP emission ratio (R=F480/F535). Emission intensities and ratios were normalized to averaged baseline signals and are given as ΔF/F and ΔR/R, respectively. Note that changes of ΔR/R indicate changes of the intracellular cGMP concentration. Based on in-cell calibration of cGi500 in permeabilized vascular smooth muscle cells (Thunemann et al. 2013a), the peak of the CNP-induced cGMP transient in E12.5 DRG neurons corresponds to ~0.5 µM cGMP. Representative results from ≥ 3 experiments with independent cell cultures are shown.

(E-G) The broad-spectrum PDE inhibitor IBMX potentiates the CNP-induced cGMP signal in DRG neurons. (E and F) FRET-based cGMP imaging was performed in cells that were superfused three times with 100 nM CNP (black horizontal bars in panel F), with the second CNP application in presence of 100 µM IBMX (red horizontal bar in panel F). Signals were recorded from the soma. Changes of ΔR/R reflect changes of the intracellular cGMP concentration. The signals at time points t0-t3 indicated in panel F correspond to the pictures shown in panel E. (F) Compared to baseline (t0), stimulation with 100 nM CNP (t1) leads to an elevation of the CFP/YFP emission ratio (R=F480/F535) that correlates with the intracellular cGMP concentration. After preincubation with IBMX, CNP stimulation (t2) results in ~2.5 times higher peak cGMP concentrations as compared to CNP alone. After washout of IBMX, the third CNP application (t3) leads to an increase of the cGMP concentration that is comparable to the first stimulation. Scale bar, 20 µm. (G) Summary of CNP-induced cGMP signals before, during and after incubation with IBMX. Peak areas were taken as a measure of the cGMP response and normalized to the first peak of the experiment. Data are mean±SEM (n = 6 cells); ***p<0.001.

RevisedManuscript.docx

140x171mm (300 x 300 DPI)

Figure 2

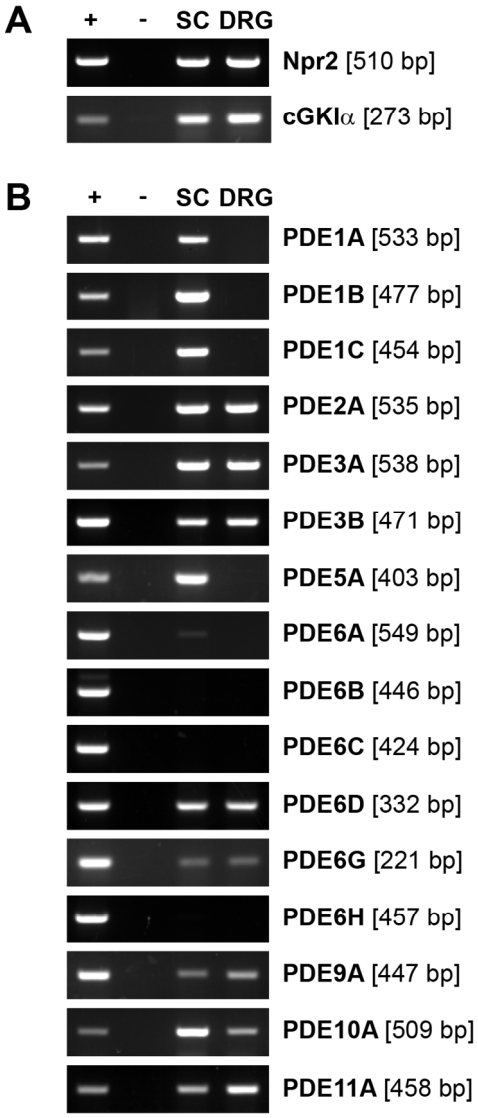

Fig. 2: ‼ ┼ ‼ ┼ Several PDEs are expressed in embryonic DRGs and spinal cord.‼ ┼ ‼ ┼ (A and B) RT-PCR screen of cGMP-specific and dual substrate-specific PDEs expressed in E12.5 DRGs or spinal cord (SC). For comparison amplification products of Npr2 and cGKIα are shown in A). The sizes of the PCR amplification products are given in parenthesis. – no template in the reaction mixture, + amplification from an embryonic mouse cDNA library.

RevisedManuscript.docx
136x349mm (300 x 300 DPI)

Figure 3

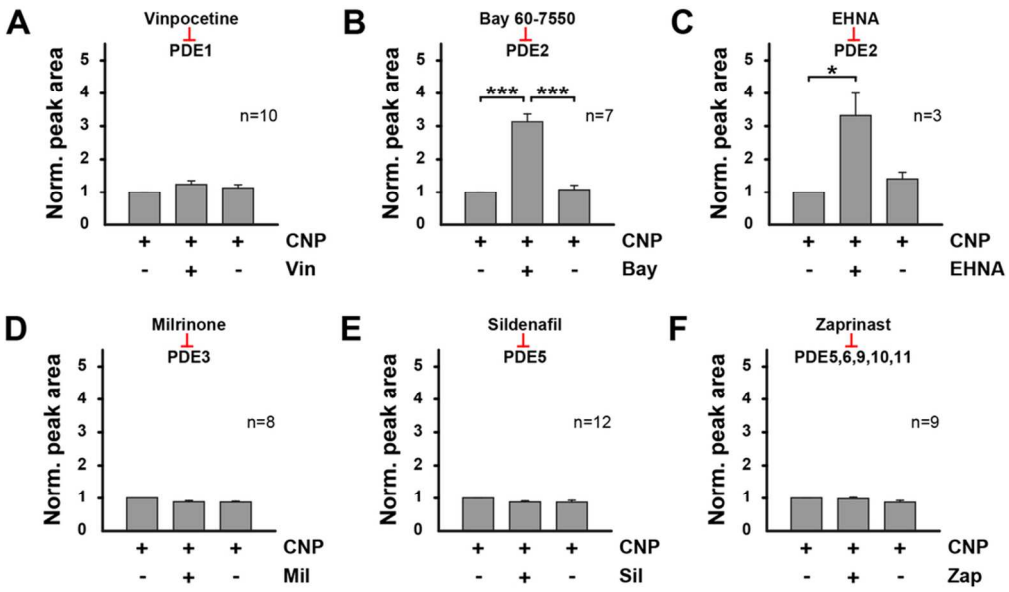

Fig. 3: ‼ ┼ ‼ ┼ Pharmacological profiling of PDE activities in DRG neurons. ‼ ┼ ‼ ┼ FRET-based cGMP imaging was used to determine the effects of various PDE inhibitors on CNP-induced cGMP signals as described in the legend to Figure 1. Cells were stimulated three times with 100 nM CNP. The second CNP stimulation was done after preincubation of the cells for 5 min with (A) 5µM vinpocetine (Vin), (B) 10 nM Bay 60-7550 (Bay), (C) 10 µM EHNA, 10 µM milrinone (Mil), (E) 20 µM sildenafil (Sil), or (F) 20 µM zaprinast (Zap). The specificity of each PDE inhibitor is indicated above each diagram. Signals were recorded from the soma. Peak areas were taken as a measure of the cGMP response and normalized to the first peak of each experiment. Data are mean±SEM (n cells in the experiment as indicated in the respective panel at the right); ***p<0.001; *p<0.05.

RevisedManuscript.docx
89x63mm (300 x 300 DPI)

Figure 4

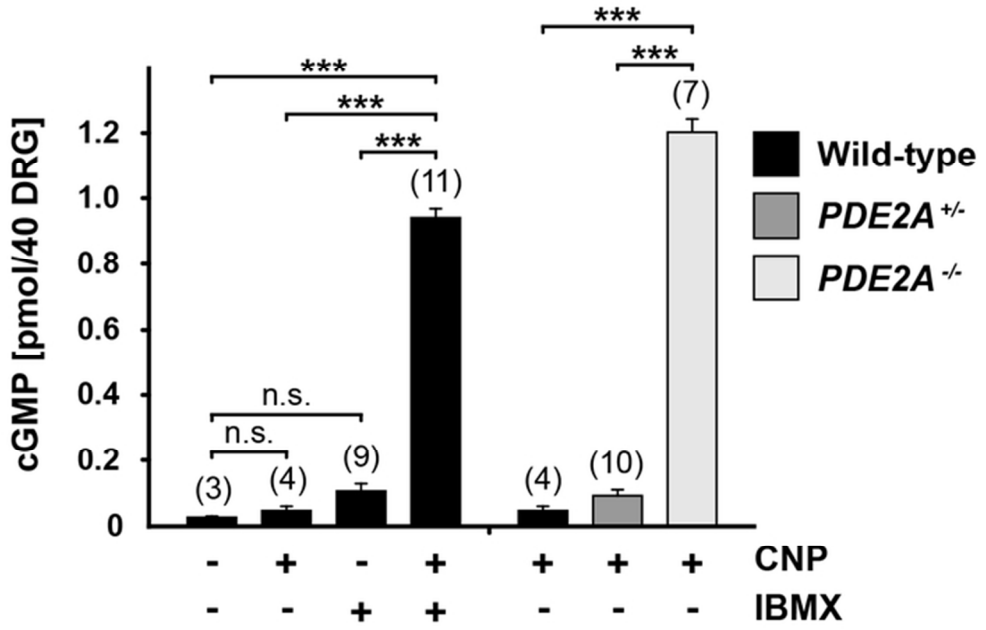

Fig. 4: ‼ ┼ ‼ ┼ PDE2A degrades CNP-induced cGMP.‼ ┼ ‼ ┼ Intact DRGs from wild type, PDE2A heterozygote or homozygous knockout mice were incubated with or without CNP-22 (0.5 µM) for 15 minutes at 37oC in the presence or absence of IBMX (1 mM). The cGMP concentration in DRG extracts was determined by an ELISA-based method as described in (Schmidt et al. 2009). Values are mean±SEM; numbers above columns indicate numbers of independent DRG preparations; t-tests were performed to compare the mean difference of two groups;*** p<0.001, n.s., non-significant.
RevisedManuscript.docx
60x46mm (300 x 300 DPI)

Figure 5

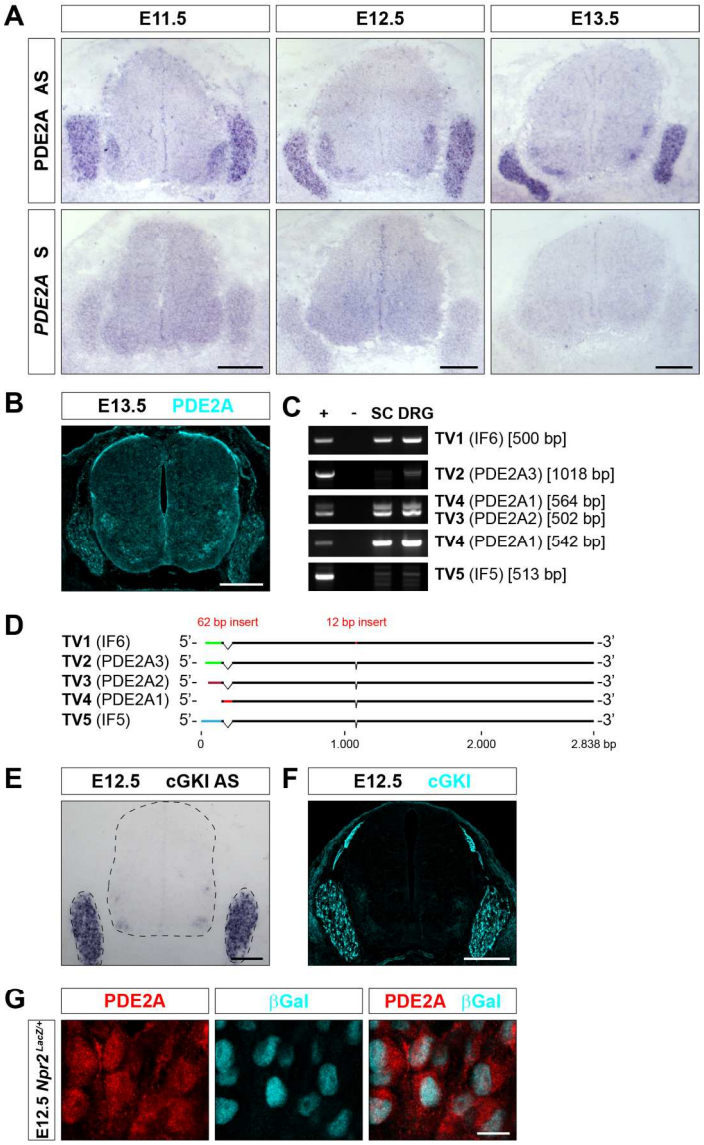

Fig. 5: ‼ ┼ ‼ ┼ Analysis of PDE2A expression in embryonic DRGs and spinal cords.‼ ┼ ‼ ┼ A) In situ hybridization of transverse sections of the spinal cord and DRGs with a PDE2A sense (S) or antisense (AS) probe reveals expression of PDE2A in DRGs and a ventrally localized pool of cells of the spinal cord. Scale bar, 200 µm. B) Immunostaining of transverse sections of the spinal cord and DRGs showing expression of PDE2A protein in DRGs, dorsal funiculus and a ventrally localized group of cells of the spinal cord. Scale bar, 200 µm. C) RT-PCR detection of PDE2A isoforms expressed in embryonic DRGs and spinal cord (SC). – no template in the reaction mixture, + amplification from an embryonic mouse cDNA library. TV, transcript variant; IF, isoform. D) Scheme of the different isoforms of PDE2A. E and F) for comparison, ISH of cGKI anti-sense probe and immunostaining of cGKI is shown. Scale bar, 200 µm. Broken lines in E) indicate the margin of the spinal cord and the DRG. G) Higher magnification of sections from an Npr2LacZ/+ reporter mouse indicates expression of PDE2A in Npr2-positive DRG neurons with nuclear labelling by an antibody to β-galactosidase. Scale bar, 10 µm.

182x315mm (300 x 300 DPI)

Figure 6

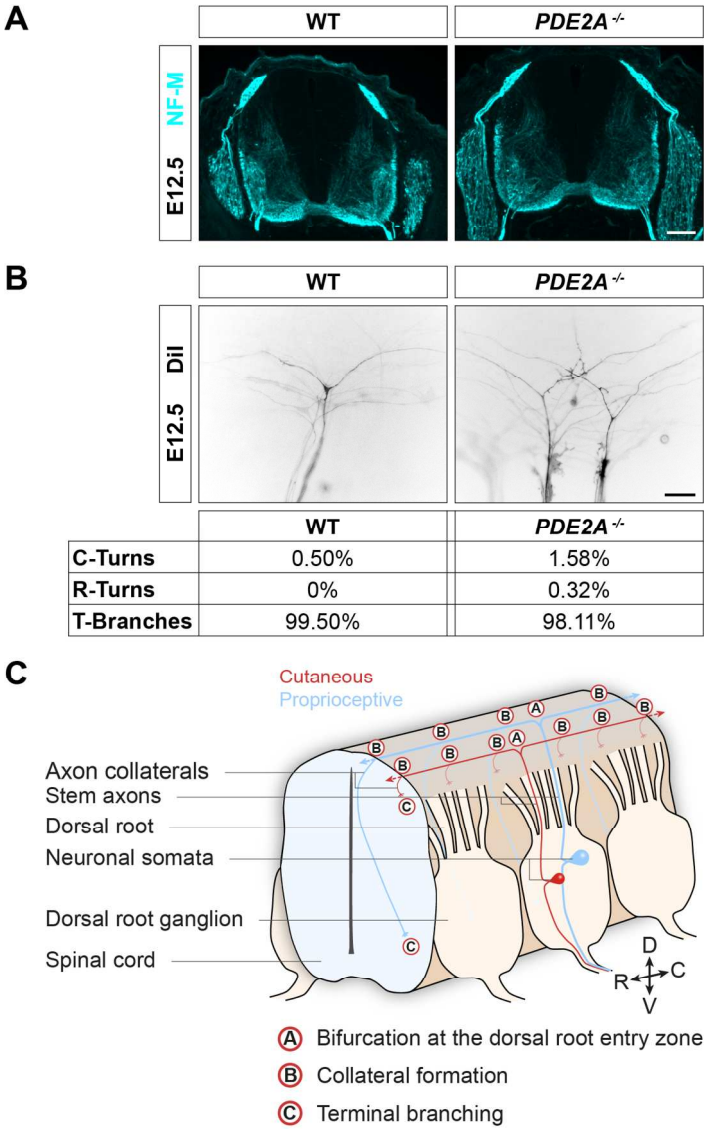

	WT	PDE2A -/-
C-Turns	0.50%	1.58%
R-Turns	0%	0.32%
T-Branches	99.50%	98.11%

Fig. 6: ‼ ┼ ‼ ┼ Analysis of sensory axon bifurcation in PDE2A mutant mice by DiI tracing.‼ ┼ ‼ ┼ A) Transversal sections of embryonic spinal cord stained with antibodies to neurofilament (NF-M) indicate that the overall structure of PDE2A-deficient spinal cord is indistinguishable from wild type spinal cord. Scale bar, 100 µm. B) DiI tracing shows that bifurcation of sensory axons is not impaired in the absence of PDE2A. 402 and 317 DRG axons were counted for wild type and for PDE2A -/-, respectively. In the right panel several PDE2A-deficient bifurcating sensory axons were labeled by DiI that are located behind the front axon. T-test indicates that the percentage of bifurcating axons in the wild type and PDE2A -/- are indistinguishable (wild type n = 3, PDE2A -/- n = 3, p = 0.123). Scale bar, 25 µm. C) Scheme of T-branching of sensory axons in the spinal cord. Sensory axons enter the spinal cord at the so-called dorsal root entry zone, bifurcate (indicated by an A) and extend at the lateral margin of the spinal cord over several segments. At more advanced stages, these stem axons form collaterals (indicated by a B) that grow to dorsal or ventral target regions of the cord where terminal branching occurs (indicated by a C).

153x263mm (300 x 300 DPI)

Figure 7

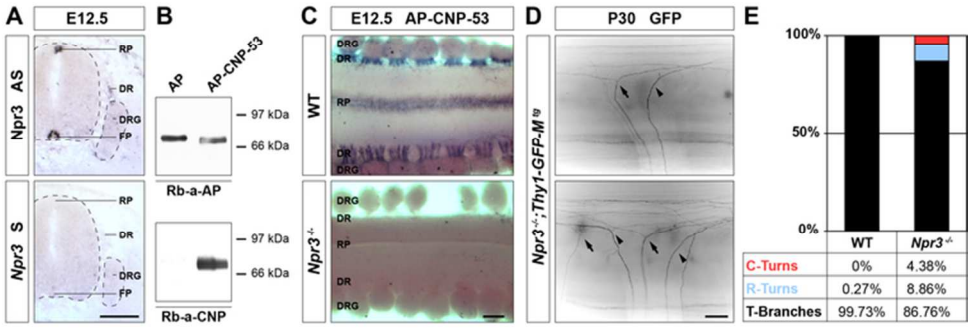

Fig. 7: ‼ ┼ ‼ ┼ Localization of Npr3 in the spinal cord and analysis of its role in axon bifurcation.‼ ┼ ‼ ┼ A) In situ hybridization using antisense (AS) and sense (S) probes to monitor Npr3 expression in transversal sections of the spinal cord reveal localization of Npr3 mRNA in the floor plate (FP), roof plate (RP) and dorsal root (DR) but not in DRGs itself. Broken lines indicate the margin of the spinal cord and the DRG. B) Expression of alkaline phosphatase (AP) or a fusion protein composed of CNP-53 and alkaline phosphatase (AP-CNP-53) in transiently tranfected COS7 cells followed by Western blotting of the resultant conditioned media using antibodies to the alkaline phosphatase (upper panel, Rb-a-AP) or to CNP (lower panel, Rb-a-CNP). The left and right lanes show expression of the alkaline phosphatase or of the fusion protein, respectively. Molecular mass standards are indicated at the right of the panels.‼ ┼ C) Detection CNP receptors in a whole-mount preparation of embryonic spinal cord using a fusion protein of CNP-53 and alkaline phosphatase (AP-CNP-53). Dorsal views demonstrate binding in dorsal roots (DR) and the roof plate (RP) of wild type embryos (upper panel), but not or only very weakly in the corresponding structures of Npr3-deficient embryos (lower panel). No staining was observed in controls with alkaline phosphatase alone (not shown). (D and E) Analysis of axon bifurcation in Npr3 knockouts crossed to the reporter mouse Thy-1-GFP-M. Spinal cords with attached DRGs were prepared at postnatal day 30 (P30). No ectopic bifurcation outside the DREZ were detected in the absence of Npr3. Arrows indicate bifurcations, arrow heads show turns in rostral or caudal directions and demonstrate the absence of bifurcations. In total 754 and 982 DRG axons were counted for wild type and Npr3-/- mutants, respectively. T-test indicates that wild type and Npr3 -/- are significantly distinct from each other (wild type n = 3, Npr3 -/- n = 8, $p<0.001$).
RevisedManuscript.docx
66x25mm (300 x 300 DPI)

Supporting information

DRG axon bifurcation tolerates increased cGMP levels: the role of phosphodiesterase 2A and scavenger receptor Npr3

Hannes Schmidt [1], Stefanie Peters [2], Katharina Frank [1, 3], Lai Wen [2], Robert Feil [2], and Fritz G. Rathjen [1]

[1] Max-Delbrück-Centrum für Molekulare Medizin in der Helmholtz-Gemeinschaft, 13092 Berlin, Germany
[2] Interfakultäres Institut für Biochemie, University of Tübingen, 72076 Tübingen, Germany
[3] Current address: Institut für Immunologie, BioMedical Center (SFB1054), Ludwig-Maximilians-Universität, 82152 Planegg-Martinsried, Germany

Key words: cyclic GMP, CNP, Npr3, Npr2, axon branching, dorsal root ganglion neurons.

Table S1. Primer sequences to amplify CNP (Nppc), Npr2, Npr3, cGKI (Prkg1) or PDE sequences from mouse tissues. TV – transcript variants, IF – isoform

Mouse Gene	**GenBank Acc. no.**	**Primer sequence**	**Product size (bp)**
Nppc	NM_010933	FOR: 5'- ACCATGCACCTCTCCCAG -3' REV: 5'- AGTGCACAGAGCAGTTCCC -3'	427
Npr2	NM_173788	FOR: 5'-TGGCGCCTTCCCCTCCTGACT-3' REV: 5'- CTGGGCCTGTTCCTGGGTTCG -3'	510
Npr3 (TV1-TV2)	NM_008728 NM_001039181	FOR: 5'- CATAGTGCGCTACATCCAAG -3' REV: 5'- CACAGAGAAGTCCCCATACC -3'	517
Pde1a	NM_016744	FOR: 5'- TCTGTACAACGACCGCTCAG -3' REV: 5'- TTGCCCCGTAGTTTGAAGAC -3'	533
Pde1b	NM_008800	FOR: 5'- CCACCCAACTAAGCAGTGGT -3' REV: 5'- TGGTTGTGCTCATCTTCTGC -3'	477
Pde1c	NM_011054	FOR: 5'- TTGACGAAAGCTCCCAGACT -3' REV: 5'- TTCAAGTCACCGTTCTGCTG -3'	454
Pde2a (TV1-TV5)		FOR: 5'- ATCCTGAACATCCCAGATGC -3' REV: 5'- GATCCCGGTAGCCTTTCTTC -3'	535
Pde2a (TV1; IF6)	NM_001143848	FOR: 5'- GGAGATTTCCCGACTTCCAG -3' REV: 5'- ACACCAATGACCTCCTGGTT -3'	500
Pde2a (TV2; Pde2a3)	NM_001008548	FOR: 5'- CGGCAGCGCGACCGGCTGAG -3' REV: 5'- TCATCTGTGAAGAAATCTCC -3'	1018
Pde2a (TV3; Pde2a2 and	NM_001143849 NM_001243757	FOR: 5'- GTCCTGGTGTTGCACCACAT -3' REV: 5'- GCAAGCTCTGTTCCTCACTG -3'	502 (Pde2a2)

TV4, Pde2a1)			564 (Pde2a1)
Pde2a (TV4; Pde2a1)	NM_001243757	FOR: 5'- CTTGCACAGAAGCCAGAACC -3' REV: 5'- TGATCTTCAGAGGCATCCACT -3'	542
Pde2a (TV5; IF5)	NM_001243758	FOR: 5'- TAGCCTTAGGAACCCAGTGC -3' REV: 5'- TGCTTCTCTACCACCTGCAA -3'	513
Pde3a	NM_018779	FOR: 5'- TGTCCCGGCCAGAGTATAAC -3' REV: 5'- CTTTCACAGGCTTCGTCCTC -3'	538
Pde3b	NM_011055	FOR: 5'- GCAAAAGATCGGGACCTACA -3' REV: 5'- ATCCACCTGCAGTTTGTTCC -3'	471
Pde5a	NM_153422	FOR: 5'- AAACATGGGACACGTGAACA -3' REV: 5'- CGCTGTTTCCAGATCAGACA -3'	403
Pde6a	NM_146086	FOR: 5'- TAAGCAAAGGCTACCGGAGA -3' REV: 5'- TCTGTACCTCCCAGGGTTTG -3'	549
Pde6b	NM_008806	FOR: 5'- TGCTGACTGTGAGGAGGATG -3' REV: 5'- CCAGAATTGAGGAGCCATGT -3'	446
Pde6c	NM_033614	FOR: 5'- GAAAGGGTACCGTCCTGTCA -3' REV: 5'- CATCTGCTCGCAGGTATCAA -3'	424
Pde6d	NM_008801	FOR: 5'- GACCTGTCTGTCCCTGGTGT -3' REV: 5'- AGCCTCACTTTGGATGTGCT -3'	332
Pde6g	NM_012065	FOR: 5'- CAAGGGTGAGATTCGGTCAG -3' REV: 5'- CGTGCAGCTCTAGGTGATTG -3'	221
Pde6h	NM_023898	FOR: 5'- ACTTACGGGAACACATTCGG -3' REV: 5'- CATGGGTCAGGGCCATATAC -3'	457
Pde9a (TV1)	NM_008804	FOR: 5'- GACGATGCCATGAAGGAGTT -3'	447

or (TV2)	NM_001163748	REV: 5'- ATTCATCCAAGGGGAAAACC -3'	444
Pde10a	NM_011866	FOR: 5'- TCCATTGAGAAAGGGATTGC -3' REV: 5'- TCAAAACAGGATGTCCCACA -3'	509
Pde11a	NM_001081033	FOR: 5'- GACCGAGGTGGAAATTTTAGC -3' REV: 5'- CTTGTTCAAAGAACTCGCTGG -3'	458
Prkg1 (α-variant)	NM_001013833	FOR: 5'- AAAAATGAGCGAACTGGAG -3' REV: 5'- GACCTCTCGGATTTAGTGAAC -3'	273
Prkg1 (α- and β-variant)	NM_001013833 NM_011160	FOR: 5'- TCGGGGAGCTGGCTATACTTTACA -3' REV: 5'- CTTCGGCTTCATATTTTGCTTTTG -3'	549
AP-CNP-53 T3		FOR: 5'- GGGCTCGAGGACCTGCGTGTGGACACC -3' REV: 5'- AATTAACCCTCACTAAAGGG -3'	287

Table S2. Statistics of FRET measurements as shown in Figure S2.

	n number	df (numerator + denominator)	F statistics (Levene's test)	P value (Bonferroni test)
Vinpocetine	10	29	1,26032	CNP1/CNP2: 0,47939 CNP2/CNP3: 1 CNP1/CNP3: 1
Bay60-7550	7	20	1,01815	CNP1/CNP2: 4,30507E-7 CNP2/CNP3: 7,06307E-7 CNP1/CNP3: 1
EHNA	3	8	7,16915	CNP1/CNP2: 0,51305 CNP2/CNP3: 0,72658 CNP1/CNP3: 1
Milrinone	8	23	0,19115	CNP1/CNP2: 1 CNP2/CNP3: 1 CNP1/CNP3: 1
Sildenafil	12	35	0,15948	CNP1/CNP2: 1 CNP2/CNP3: 1 CNP1/CNP3: 1
Zaprinast	9	26	2,38858	CNP1/CNP2: 1 CNP2/CNP3: 1 CNP1/CNP3: 0,97735
IBMX	6	17	1,0056	CNP1/CNP2: 3,28141E-6 CNP2/CNP3: 1,00787E-6 CNP1/CNP3: 1

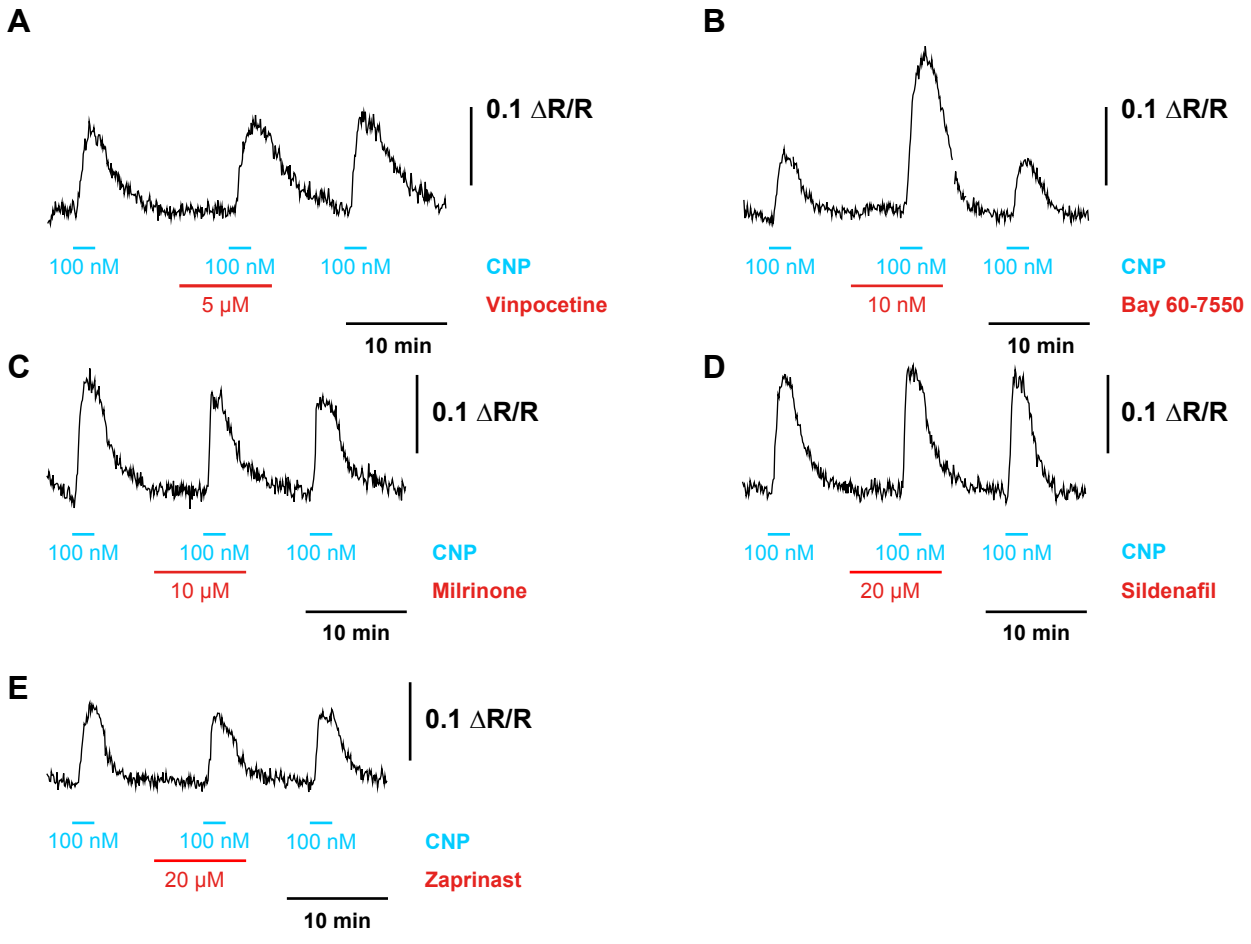

Fig. S1: Single traces of FRET measurements using different PDE inhibitors. DRG neurons were superfused three times with 100 nM CNP (black horizontal bars), with the second CNP application in the presence of a PDE inhibitor (red horizontal bar) given at the indicated concentration. Signals were recorded from the soma. Changes of ΔR/R reflect changes of the intracellular cGMP concentration. Preincubation with PDE inhibitors before the application of CNP did not affect the cGMP levels.

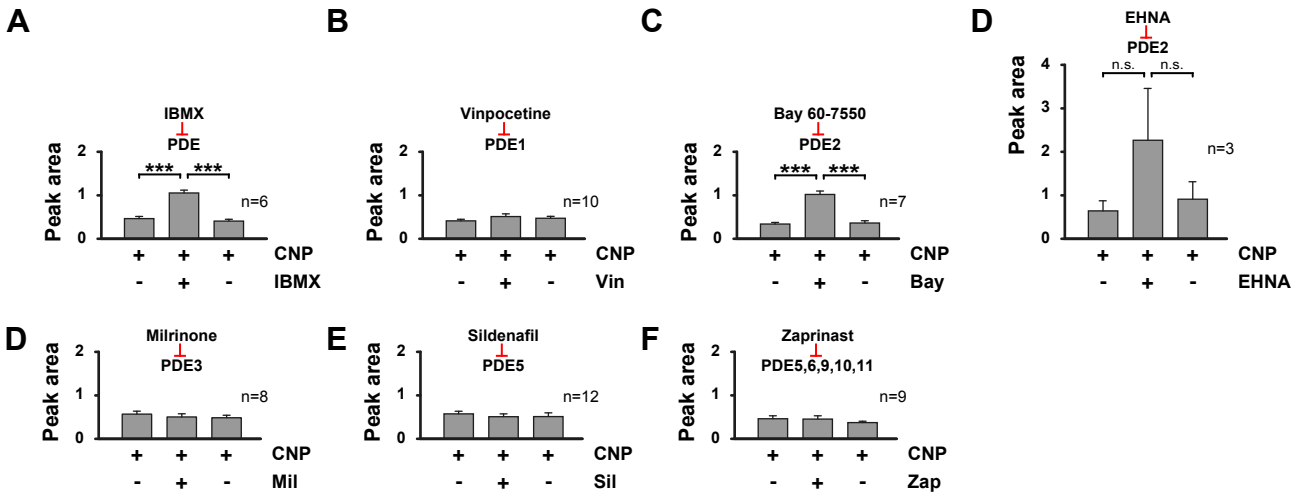

Fig. S2: Pharmacological profiling of PDE activities in DRG neurons. Non-normalized values of Figure 3 (main text) are shown. The statistical analysis is summarized in table S2 of the supporting information. Cells were stimulated three times with 100 nM CNP. The second CNP stimulation was done after preincubation of the cells with (A) 5µM vinpocetine (Vin), (B) 10 nM Bay 60-7550 (Bay), (C) 10 µM EHNA, 10 µM milrinone (Mil), (E) 20 µM sildenafil (Sil), or (F) 20 µM zaprinast (Zap). The specificity of each PDE inhibitor is indicated above each diagram. Signals were recorded from the soma. Peak areas were taken as a measure of the cGMP. Data are mean±SEM;*** $p<0.001$; n.s., non- significant.

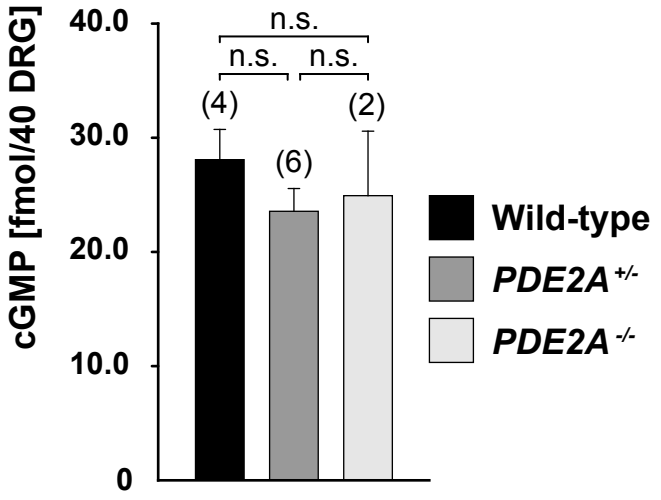

Fig. S3: Intact DRGs from wild type, PDE2A heterozygote or homozygous knockout mice were incubated with or without CNP-22 (0.5 µM) for 15 minutes at 37oC. The cGMP concentration in DRG extracts was determined by an ELISA-based method as described in (Schmidt et al. 2009). Bars indicate SEM; numbers above columns indicate numbers of independent DRG preparations; t-tests were performed to compare the mean difference of two groups. n.s., non-significant.

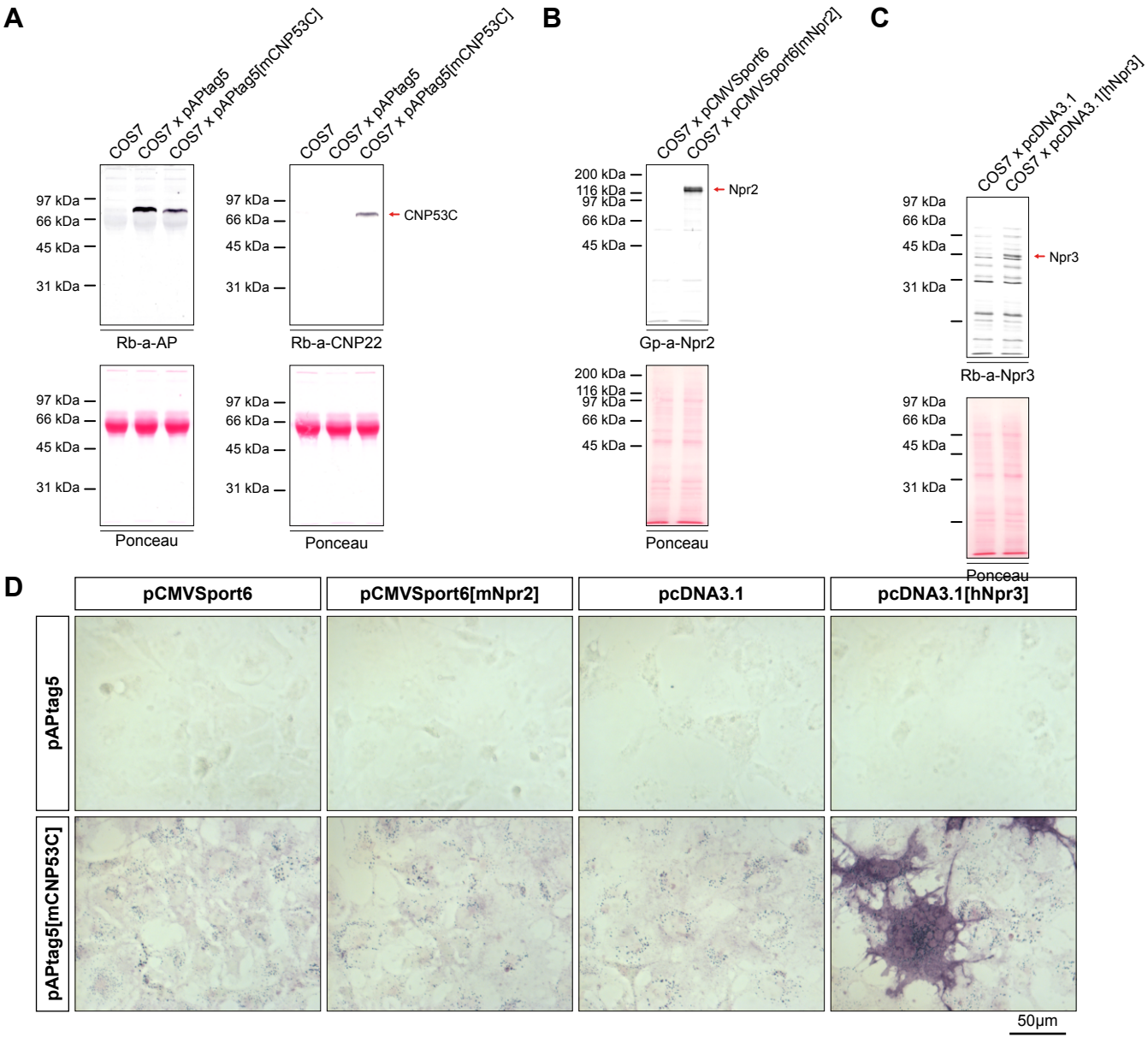

Fig. S4: Analysis of AP-CNP-53 binding to heterologous cells. (A) Western blotting demonstrating detection of AP-CNP-53 in the supernatants of transiently transfected COS7 cells which was used for binding to Npr3 expressed in COS7 cells (D) or in whole mounts of spinal cord (see Figure 7C). The vector encoding alkaline phosphatase or untransfected COS7 cells served as control. Equal protein loading is demonstrated by Ponceau staining. Rabbit antibodies to the alkaline phosphatase (GenHunter Corp, Q301) were used at a dilution of 1: 2500 and rabbit antibodies to CNP22 (Peninsula Lab. Inc, T-4223) were applied at a dilution 1:2000. Goat anti-rabbit alkaline phosphatase (Dianova, 1:4000) and donkey guinea pig (Dianova, 1:4000) were used as secondary antibodies. (B) Western blotting demonstrating expression of mouse Npr2 in transfected COS7 cells. Equal protein loading is demonstrated by Ponceau staining. Guinea pig antibodies to mNpr2 have been described elsewhere and were used at a dilution of 1:5000 (Ter-Avetisyan et al. 2014). Molecular mass markers are to the left of each panel. (C) Western blotting demonstrating expression of human Npr3 in tranfected COS7 cells. Equal protein loading is demonstrated by Ponceau staining. Rabbit antibodies to Npr3 were from Abcam (ab37617) and diluted at 1 µg/ml. Molecular mass markers are to the left of each panel. (D) Binding of AP-CNP-53 (pAPtag5[mCNP53C]) to COS7 cells transiently transfected with plasmids encoding Npr2 or Npr3. Strong binding is observed to Npr3 whereas no signals above background were detected in Npr2 expressing cells. Specificity is demonstrated by applying the alkaline phosphatase alone (pAPtag5). The fusion protein AP-CNP-53 and the alkaline phosphatase were collected from COS7 supernatants (see A) and diluted 1:4 in medium.

Expression of phosphodiesterase 2A in embryonic DRG neurons and localization of Npr3 in the dorsal roots, the roof plate and lining the floor plate is shown. Their influence on intracellular cGMP levels and their role in axon bifurcation of DRG neurons in PDE2A or Npr3 mutants was analyzed.

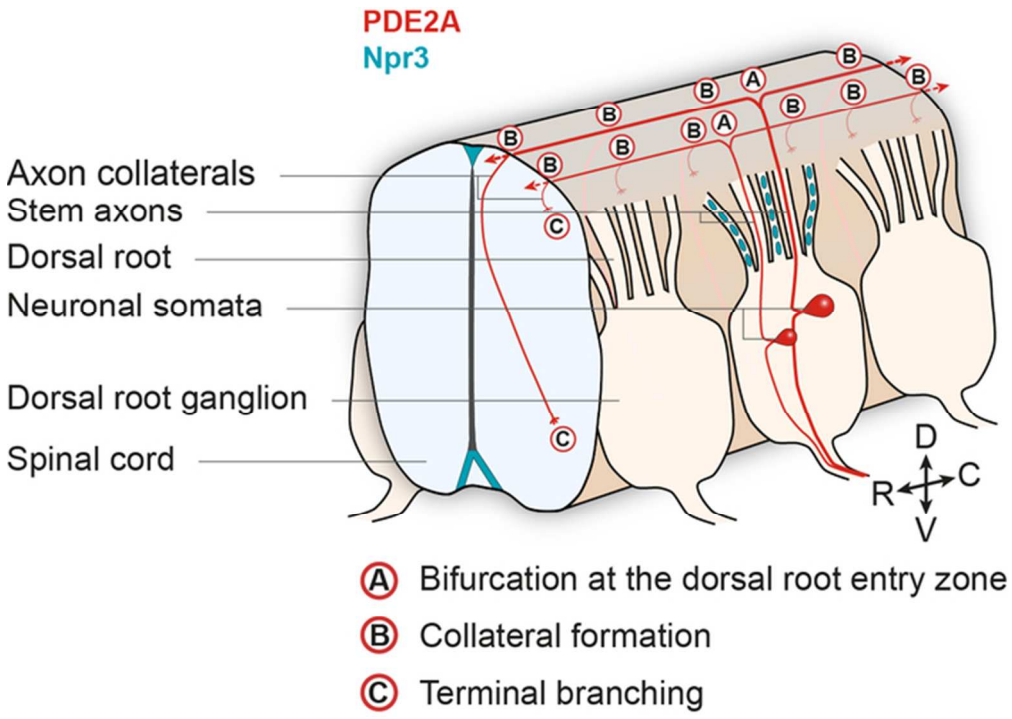

Expression of phosphodiesterase 2A in embryonic DRG neurons and localization of Npr3 in the dorsal roots, the roof plate and lining the floor plate is shown. Their influence on intracellular cGMP levels and their role in axon bifurcation of DRG neurons in PDE2A or Npr3 mutants was analyzed.

59x42mm (300 x 300 DPI)